



# Contrail formation within cirrus: high-resolution simulations using ICON-LEM

Pooja Verma<sup>1,2</sup> and Ulrike Burkhardt<sup>1</sup>

<sup>1</sup>Deutsches Zentrum für Luft- und Raumfahrt, Institut für Physik der Atmosphäre, Oberpfaffenhofen, Germany

5 <sup>2</sup>Formerly at Meteorologisches Institut, Ludwig-Maximilians-Universität, Munich, Germany

Correspondence to: Pooja Verma ([Pooja.Verma@dlr.de](mailto:Pooja.Verma@dlr.de)) and Ulrike Burkhardt ([Ulrike.Burkhardt@dlr.de](mailto:Ulrike.Burkhardt@dlr.de))

**Abstract.** Contrail formation within natural cirrus introduces large perturbations in cirrus ice crystal number concentrations leading to modifications in cirrus microphysical and optical properties. The number of contrail ice crystals formed in an aircraft plume depends on the atmospheric state and aircraft and fuel properties. Our aim is to study the impact of pre-existing cirrus  
10 on the contrail formation processes. We analyze contrail ice nucleation within cirrus and the survival of contrail ice crystals within the vortex phase and their change due to the presence of cirrus ice crystals within the high-resolution ICON-LEM at a horizontal resolution of 625m over Germany.

We have selected two different synoptic situations sampling a large range of cirrus cloud properties from very thick cirrus connected with a frontal system to very thin cirrus within a high-pressure system. We find that contrail formation within cirrus  
15 often leads to increases in cirrus ice crystal numbers by a few orders of magnitude. Pre-existing cirrus has an impact on contrail ice crystal number concentrations only if the cirrus is optically thick. In thick cirrus, contrail ice nucleation rates and ice crystal survival rates within the vortex phase are both increased. The sublimation of the cirrus ice crystals sucked into and subsequently sublimated within the aircraft's engine leads to an increase in the contrail formation threshold by up to 0.7K which causes an increase in the number of nucleated contrail ice crystals. This increase can be large at lower flight levels where ambient  
20 temperatures are close to the contrail formation threshold temperature and when the ice water content of the pre-existing cirrus cloud is large. During the contrail's vortex phase the aircraft plume is trapped within the descending vortices in which the decrease in plume relative humidity leads to the sublimation of contrail ice crystals. This contrail ice crystal loss can be modified by the cirrus ice crystals that are mixed into the plume before the start of the vortex phase. In particular, high ice crystal number concentrations and large ice water content of the pre-existing cirrus cloud or low contrail ice crystal numbers  
25 are associated with significant increases in the contrail ice crystal survival rates.

## 1 Introduction

Cirrus clouds are very common in the upper troposphere and have a large impact on radiative transfer and, therefore, on climate and weather (Liou, 1986). Cirrus cool the atmosphere by reflecting incoming short-wave (solar) radiation and absorb and re-emit outgoing long-wave (terrestrial) radiation which warms the atmosphere. The size of both the short-wave and long-wave



30 cloud radiative forcing depends on the macro- and microphysical cirrus properties (Ramanathan et al., 1989; Zhang et al.,  
1999). Aviation has a significant impact on upper tropospheric cirrus cloudiness (Boucher, 2013) due to the formation of  
contrails and due to aviation aerosol cloud interactions. Of the known aviation related radiative forcing components contrail  
cirrus is estimated to be the largest (Burkhardt and Kärcher, 2011) but the associated uncertainty is large (Lee et al., 2021).  
This is not unexpected since in IPCC style double CO<sub>2</sub> climate change simulations uncertainties in cloud responses are the  
35 main source of uncertainty in the equilibrium climate sensitivity (Stevens and Bony, 2013). In assessments of aviation related  
climate change (Lee et al., 2021) contrail cirrus and the indirect aerosol effects involving aviation aerosol emissions are the  
most notoriously difficult to estimate and the most uncertain (e.g. Righi et al., 2013, Kapadia et al., 2016, Lee et al., 2021)  
with uncertainties caused to a large degree by incomplete knowledge about number and ice nucleating properties of emitted  
and subsequently ageing aviation aerosols.

40 Contrail cirrus have been studied in great detail in observations (e.g. Gayet et al., 1996, Schröder et al., 1999, Voigt et al.,  
2017, Schumann et al., 2017) and in modelling. Modelling the life cycle of contrail cirrus, just as modelling natural clouds,  
involves processes on a large range of scales, comprising microphysical processes as well as large scale dynamics. Different  
approaches have been used, ranging from simulating single contrails over parts or the whole life cycle in LES (e.g. Lewellen  
et al., 2014, Unterstrasser, 2014, Paoli and Shariff, 2016) or NWP (Gruber et al., 2018) to simulating the evolution, properties  
45 and the climate impact of a large number of contrails in low resolution models with a significantly simplified microphysical  
treatment (Burkhardt and Kärcher, 2011; Bock and Burkhardt, 2016a, 2016b, 2019; Bier et al., 2017; Chen and Gettelman,  
2013; Schumann et al., 2015). While LES is ideally suited to resolving the flow field around the airplane and, therefore, the  
contrail evolution in the first few minutes, numerical weather prediction and climate models are suited to simulating the contrail  
evolution which depends on the evolving atmospheric conditions controlled by synoptic scale variability.

50 Despite those efforts understanding contrail cirrus processes, many uncertainties connected with the background upper  
tropospheric water budget and cirrus cloud properties, the contrail cirrus schemes and the impact of contrail cirrus on radiative  
transfer remain (Lee et al., 2021). Furthermore, the interaction between contrail cirrus and natural cirrus add to the uncertainty.  
Upper tropospheric natural cloudiness has been shown to decrease as a consequence of contrail formation and is, therefore,  
limiting the impact of contrail formation on climate (Burkhardt and Kärcher, 2011; Schumann et al., 2015; Bickel et al., 2020).

55 The strength of this cloud adjustment is very uncertain. Furthermore, until now only contrail formation within a previously  
cloud-free air volume has been studied extensively. The impact of contrail formation within pre-existing clouds is largely  
unknown because it was thought to be secondary or even negligible. Contrail induced cloud perturbations within existing cirrus  
have recently been shown to lead to changes in cloud optical depth that can be detected using satellite remote sensing (Tesche  
et al., 2016) which calls into question the assumption that this effect is negligible.

60 Contrails form when relative humidity within the aircraft exhaust plume exceeds saturation relative to water as a consequence  
of the mixing of the plume air with ambient air (Schumann, 1996). Contrail formation is subject to the atmospheric state and  
aircraft and fuel parameters. The number of ice crystals nucleated during contrail formation depends on the thermodynamic  
state of the ambient atmosphere and on aircraft and fuel parameters, in particular the number of aerosol particles released by



the engine (Kärcher et al., 2015). At cruise altitude in the mid latitudes the atmospheric state is such that the number of emitted  
65 aerosol particles constrains the number of ice crystals forming within the contrail's jet phase (Bier and Burkhardt, 2019). At  
lower latitudes or altitudes this is not necessarily the case; here the thermodynamic state of the ambient atmosphere, which is  
responsible for the evolution of relative humidity in the plume, often limits ice nucleation within contrails. Within the  
subsequent vortex phase, that lasts until a few minutes after emission, the aircraft induced wake vortices travel downwards  
and many of the contrail's ice crystals that are trapped within the vortices sublime depending on the atmospheric state,  
70 aircraft parameters and the number of contrail ice crystals that nucleated within the jet phase (Unterstrasser, 2016).

Both, ice nucleation in the jet phase and ice crystal survival during the vortex phase may be modified by the existence of ice  
crystals from pre-existing clouds. Ice crystals from pre-existing cirrus that are sucked into the engine sublime and lead to a  
small increase in the water vapor content of the plume (Gierens, 2012). This can in turn lead to a small change in the contrail  
formation criterion and in contrail ice nucleation. Before the aircraft plume is trapped within the wake vortices ambient air  
75 mixes with the plume air which leads to the presence of cirrus ice crystals within the aircraft plume. During vortex descent  
both cirrus and contrail ice crystals can sublime. The sublimation of the cirrus ice crystals increases the relative humidity  
within the vortex and can lead to a change in the fraction of contrail ice crystals surviving the vortex loss. Any modification  
of the ice nucleation or survival during the vortex phase leading to changed ice crystal numbers after the vortex phase has an  
impact on contrail microphysical processes, contrail cirrus properties, optical depth and life time (Bier et al., 2017; Burkhardt  
80 et al., 2018). Increased ice crystal numbers lead to a stronger climate impact of contrail cirrus. Previous rough estimates of the  
impact of pre-existing ice crystals on contrail formation hint at the influence of the pre-existing clouds to be negligible  
(Gierens, 2012). We choose an approach in between LES and a global climate model, studying contrail formation in a  
numerical weather prediction setup at a resolution of a few hundred meters. We consider a wide range of cirrus cloud properties  
as simulated by ICON-LEM, calculating changes in the contrail formation criterion and in the number of ice crystals nucleating  
85 during contrail formation and in the contrail ice crystal loss during the vortex phase.

We use the high-resolution ICON-LEM in weather forecasting mode (Heinze et al., 2017) to study contrail formation within  
pre-existing clouds in detail. In section 2 we introduce the ICON model and describe the contrail related processes that are part  
of our contrail scheme. The scheme consists of a parameterization for ice nucleation and for the ice crystal loss in the contrail's  
vortex phase and additions that consider the existence of pre-existing ice crystals from natural cirrus and simulates contrail  
90 evolution starting after the contrail's vortex phase. We study contrail formation processes on two selected days that represent  
different synoptic situations over Germany and discuss the background natural cirrus cloud properties (Sect. 3.1). We analyze  
contrail ice nucleation within cirrus and the impact of pre-existing cirrus clouds on contrail formation threshold and ice  
nucleation (Sect. 3.2) and on the contrail ice crystal survival in the vortex phase (Sect. 3.3).



## 2 Methods and Simulations

95 We develop and implement a representation for contrail ice nucleation in the jet phase and ice crystal loss during the contrail's  
vortex phase in the ICON (ICOsahedral Non-hydrostatic) - LEM (Zängl et al., 2014; Dipankar et al., 2015) that allows to study  
cirrus cloud modifications induced by contrail formation. We use a model set up that simulates the synoptic development over  
a limited domain, Germany, at a horizontal resolution of 625m using initial and boundary data coming from an operational  
NWP system, COSMO (COntortium for Small-scale MOdelling, Baldauf et al., 2011), at 2.8 km resolution. Instead of  
100 prescribing an air traffic inventory, we prescribe air traffic everywhere in the upper troposphere studying the impact of pre-  
existing clouds on contrail formation, the contrail formation temperature threshold, ice nucleation and ice crystal loss in the  
vortex phase, for a large range of atmospheric states and cloud properties. We intentionally prescribe also air traffic at low  
altitudes down to about 7 km, that are usually not thought of as main air traffic levels, as air space over Germany has become  
very tight in the last years and more short distance flights have been moved to lower flight levels. Furthermore, vertical shifts  
105 in air traffic are being discussed in connection with the mitigation of aviation climate impacts (Fichter et al., 2005, Matthes et  
al., 2021).

### 2.1 ICON-LEM

ICON-LEM is based on the ICON (ICOsahedral Non-hydrostatic) modelling framework developed by the German Weather  
Service (DWD) and the Max-Planck Institute for Meteorology (Zängl et al., 2015, Dipankar et al., 2015). ICON solves a set  
110 of equations on an unstructured triangular grid based on successive refinement of a spherical icosahedron (Wan et al., 2013,  
Zängl et al., 2015). Time stepping is performed using a predictor-corrector scheme. A summary of the model configuration  
and a description of the physics package are given in Heinze et al., (2017) and references therein.

We use ICON in a LEM (large-eddy modelling) mode over Germany with realistic orography at a resolution of 625m and a  
time step of 3 seconds (Dipankar et al., 2015). The model has an option for 2 one-way nested domains. The model's high  
115 horizontal resolution combined with a vertical resolution of around 150m in the upper troposphere allows resolving relevant  
cloud processes, such as convection, while cloud microphysics, turbulence and radiation remain parameterized. Resolved cloud  
scale dynamics lead to improvements in structure and distribution of clouds and precipitation (Stevens et al., 2021). The  
heterogeneity in the cloud field and thus in the optical depth is largely resolved which enables a more realistic estimation of  
the radiative forcing relative to coarser resolution models. The model is initialized at 00 UTC from operational COSMO-DE  
120 analysis data (Baldauf et al., 2011) and relaxed at the lateral boundaries within a 20km nudging zone towards COSMO-DE  
analysis which are updated hourly. The initial and boundary condition data are interpolated to the ICON grids by using a radial  
basis function (RBF) interpolation algorithm (Ruppert, 2007) and 3D variables are interpolated vertically during initialization.  
An evaluation of the model simulations has been presented by Heinze et al., (2017) and Stevens et al., (2020). The benefit of  
the high resolution of ICON-LEM or ICON-SRM (Storm Resolving Model) relative to lower resolution simulations was shown  
125 to lead to improvements in precipitation patterns, their location, propagation and diurnal cycle, and cloud properties, in



particular the vertical structure and diurnal cycle (Stevens et al., 2020). In order to minimize computing time and disk space, we choose to run the model at 625m horizontal resolution. The benefit from increasing resolution from 625m to 156m was shown by Stevens et al., (2020) to be small.

### 2.1.1 Two moment cloud microphysics

130 The cloud microphysical scheme of ICON-LEM is based on Seifert and Beheng (2006) and includes microphysical processes  
in liquid, mixed phase and ice phase clouds. The microphysical two-moment scheme predicts mass mixing ratios and number  
concentrations for six hydrometeors, cloud droplets, rain, ice, hail, snow, and graupel. The cloud cover scheme is an all-or-  
nothing scheme disregarding subgrid variability of total water. The microphysical scheme describes droplet formation and ice  
nucleation, growth and conversion processes between different hydrometeors, precipitation, and sedimentation. The  
135 parameterization for homogeneous and heterogeneous ice nucleation is based on Kärcher et al., (2006) and includes the  
competition between homogeneous and heterogeneous nucleation, and considers the impact of pre-existing ice crystals.  
Heterogeneous nucleation is induced by INPs (Ice nucleating particles) with mineral dust concentrations prescribed according  
to Hande et al., (2015). Activation of INPs for heterogeneous nucleation is parameterized based on the simulation of the aerosol  
conditions with the COSMO MultiScale Chemistry Aerosol Transport (COSMO-MUSCAT) model (Wolke et al., 2004, 2012).  
140 A tracer is used to track the number of ice nuclei that have formed ice crystals and are therefore not available for ice nucleation  
anymore (Köhler and Seifert 2015).

### 2.2 Contrail scheme

We developed and implemented a contrail scheme within ICON-LEM to study changes in cloud variables due to contrail  
formation. Contrail formation, dependent on atmospheric and aircraft and fuel parameters, is calculated and contrail ice  
145 nucleation (Sect. 2.2.1) and ice crystal loss in the contrail's vortex phase (Sect. 2.2.3) is estimated. Contrail ice crystals are  
distributed vertically consistent with the maximum displacement of the vortices which is dependent on the state of the  
background atmosphere and on aircraft properties (Sect. 2.2.3). We analyze contrail ice crystal number concentrations after  
the contrail's vortex phase at a contrail age of ~5 minutes. If contrails form within a pre-existing cirrus, the cirrus can have an  
impact on the contrail formation threshold, contrail ice nucleation and contrail ice crystal survival during the vortex phase  
150 depending on the cirrus macro- and microphysical properties. We consider the impact of the sublimation of natural cirrus ice  
crystals that are sucked into the combustor and lead to a slight increase in water vapor mixing ratio in the young plume and  
increase on the contrail formation threshold temperature and contrail ice nucleation (Sect. 2.2.2). After contrail ice nucleation,  
water vapor deposition leads to an increase in the sizes of the contrail and cirrus ice crystals, that were mixed into the plume,  
dependent on the size of the respective ice crystals. We consider the impact of the sublimation of ice crystals from the pre-  
155 existing cirrus, that are mixed into the young plume and are caught in the descending wake vortices, on the water vapor mixing



ratio within the descending vortex. The sublimation of the cirrus ice crystals increases relative humidity within the vortex and reduces the sublimation of contrail ice crystals (Sect. 2.2.4).

In order to sample through a large number of atmospheric states with varying cloud properties without having to perform long simulations we pick two different synoptic situations with very different background conditions and cloud properties. Both situations are part of one-day long ICON-LEM simulations described in Heinze et al., (2017). For each of those situations we study contrail formation in the upper troposphere (above ~7 km) for only one timestep prescribing air traffic in each grid box of the simulation domain.

### 2.2.1 Parameterization of contrail formation and ice nucleation

Contrail formation depends on atmospheric conditions and fuel and aircraft dependent parameters and is described by the Schmidt-Appleman (SA)-criterion (Schumann, 1996). The temperature threshold for contrail formation depends on the slope of the mixing line,  $G$ , in a temperature-water vapor partial pressure diagram:

$$G = \frac{M_w c_p P_a}{0.622 Q (1-\eta)}, \quad (1)$$

with  $M_w$ ,  $c_p$ ,  $P_a$ ,  $Q$  and  $\eta$  are mass emission index of water vapor, specific heat capacity, atmospheric pressure, combustion heat and propulsion efficiency, respectively. We set the mass emission of water vapor to  $1.24 \text{ kg (kg-fuel)}^{-1}$ , combustion heat to  $43.2 \text{ MJ (kg-fuel)}^{-1}$ , and propulsion efficiency to 0.3 (Bock and Burkhardt, 2019). The temperature threshold of contrail formation,  $T_{sa}$ , is the ambient temperature for which the slope of the water saturation curve is equal to  $G$ , the slope of the plume mixing line. At ambient temperatures below that threshold, contrails will form if the ambient humidity is high enough. Contrails will only persist if ambient humidity is at least saturated relative to ice. At a given pressure level and for a given propulsion efficiency the slope of the mixing line depends on the ratio of emitted water vapor and combustion heat. An increase in water vapor emissions at constant combustion heat therefore leads to an increase in the slope of the mixing line and therefore to a higher temperature threshold of contrail formation.

Ice nucleation takes place within the first second after emission in the contrail's jet phase (Paoli and Shariff, 2016). The hot and moist air of the plume rapidly mixes with the cold and dry ambient air. If water saturation is exceeded within the plume, droplets form preferentially on emitted soot particles and background aerosols (Kärcher and Yu, 2009; Kärcher et al., 2015). The number of droplets that form within the contrail is dependent on the supersaturation and the size distribution and hygroscopicity of the aerosols. At current soot number emissions, volatile plume particles are generally too small to get activated. Once droplets have formed in the plume they rapidly freeze into ice particles by homogeneous freezing when plume temperatures fall below the freezing temperature. If the contrail formation threshold temperature is close to the ambient temperature then the maximum attainable plume supersaturation (when neglecting the decrease in supersaturation due to droplet formation) will be low and, therefore, only few soot particles will activate into water droplets and subsequently freeze (Kärcher and Yu, 2009, Kärcher et al., 2015). Close to the temperature threshold the apparent emission index ( $AEI_i$ ) of contrail



ice crystals increases rapidly with decreasing ambient temperature,  $T_a$ . Contrail formation close to the contrail formation threshold occurs often at low air traffic altitudes where air is relatively warm or in tropical or subtropical areas (Bier and Burkhardt, 2019). When contrails form far below the contrail formation threshold,  $AEI_i$  is controlled by the soot number emission index. As ambient temperature decreases maximum attainable plume supersaturation increases and an increasing number of soot particles can activate and form ice crystals. The number of soot particles forming ice crystals is for temperatures 5K below the formation threshold close to the number of emitted soot particles (within approximately 25%). This means that in the extratropics at typical cruise levels ice crystal numbers in young contrails are mostly limited by the number of emitted soot particles (Bier and Burkhardt, 2019).

195 We have implemented the parameterization of contrail ice nucleation based on Kärcher et al., (2015). The parameterization calculates the number of droplets that form and subsequently freeze within the contrail's jet phase. The number of droplets that form within the contrail is determined by calculating the number of droplets that can form at a given plume supersaturation and that lead to a decrease in relative humidity that balances the large increase in relative humidity due to the mixing of plume and environmental air. All aerosols are assumed to activate and form droplets at the same time,  $t_o$ , called the "activation-  
200 relaxation time" neglecting the fact that aerosols that activate slightly earlier would have an impact on the plume relative humidity.

We have calculated the apparent emission index of contrail ice crystals ( $AEI_i$ ) prescribing a soot emission index (EIs), assuming current day soot rich emissions of  $2.5 \times 10^{15}$  soot particles per kg-fuel, on model levels between 7 km to 13 km altitudes. Figure 1 shows the dependency of  $AEI_i$  on the difference between the ambient and the threshold temperature in the  
205 altitude range between 9.6 to 10.8 km for varying atmospheric conditions. Close to the formation threshold ( $T_{sa}-T_a < 3K$ )  $AEI_i$  rapidly increases with increasing difference between ambient temperature and the temperature threshold for contrail formation. At ambient temperature far below the temperature threshold a large percentage of the soot particles activate and form contrail ice crystals so that  $AEI_i$  approaches EIs. The apparent emission index of ice varies for fixed difference between ambient and Schmidt-Appleman temperature since atmospheric conditions, i.e. pressure, water vapor mixing ratio and the Schmidt-  
210 Appleman temperature, are not constant.



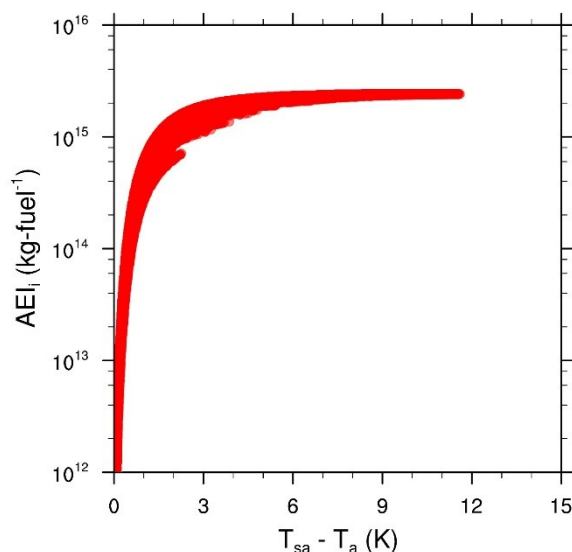


**Figure 1: Apparent Emission Index,  $AEI_i$  versus the difference between ambient temperature,  $T_a$ , and Schmidt-Appleman temperature,  $T_{sa}$ , for the 26<sup>th</sup> April 2013 at altitudes between 9.6km to 10.8km for varying atmospheric pressure, ice saturation ratio and temperature threshold for contrail formation.**

### 2.2.2 Impact of natural cirrus sublimation on contrail formation and ice nucleation

Contrail formation within pre-existing cirrus is very similar to formation in cloud free air. The end point of the plume mixing line is given by the ambient temperature and the in-cloud water vapor partial pressure. The slope of the mixing line (equation 1) is modified by the presence of the cirrus ice crystals that are sucked into the aircraft engine together with the ambient air and sublimates. Assuming a mass-based air to fuel mixing factor at engine outlet,  $N_0$ , of  $70 \text{ kg-air (kg-fuel)}^{-1}$ , we estimate the sublimated ice water content per kg-fuel,  $iwc_{sub}$ :

$$iwc_{sub} = iwc_{ci} * N_0 \quad (2)$$

with  $iwc_{ci}$  the ice water content of cirrus ( $\text{kg (kg-air)}^{-1}$ ). When calculating the slope of the plume's mixing line we add the  $iwc_{sub}$  to the mass emission index of water vapor,  $M_w$ . The new slope for the mixing line  $G_{ci}$  is:

$$G_{ci} = \frac{(M_w + iwc_{sub})c_p P_a}{0.622Q(1-\eta)} \quad (3)$$

The slope of the mixing line  $G_{ci}$  increases slightly due to the sublimation of the background cirrus ice crystals. This increase in the slope of the mixing line leads to an increase in the temperature threshold for contrail formation. This means that plume supersaturation can occur earlier and the maximum attainable relative humidity, that is reached within the plume when neglecting the decrease in supersaturation due to droplet formation, can be larger. Therefore, ice nucleation can be increased.





### 2.2.3 Parameterization of ice crystal loss during vortex descent

A few seconds after the emission, the exhaust plume including the newly formed ice crystals gets trapped in a pair of counter rotating vortices (primary wake) that are created when the vorticity sheet originating from the pressure differences at the aircraft wings rolls up (Paoli and Shariff, 2016). The counter rotating vortices propagate downward depending on atmospheric stability and aircraft properties, such as weight, wing span and speed (Gerz et al., 1998). The density contrast between the air in the vortex, that descends through a stably stratified atmosphere, and the surrounding creates vorticity that is shed upwards (secondary wake) and part of the exhaust, between 10% and 30% (Gerz et al., 1998), are detrained into the secondary wake. The secondary wake stays close to the flight level. The primary wake often descends a few hundred meters. Many ice crystals within the primary downward propagating vortices sublime due to adiabatic heating and the associated decrease in relative humidity, while the ice crystals in the secondary wake are more likely to survive. Survival of the ice crystals in the vortex regime depends on atmospheric temperature, humidity, the number of nucleated ice crystals and the maximum vertical displacement of the vortices. After vortex descend most of the air that was forced downwards rises again creating a vertically extended contrail.

The parameterization for the impact of the vortex descent on contrail properties in ICON-LEM is based on the work of Unterstrasser (2016). He used LES to study for a number of different aircraft (with differences in weight and wing span) and varying conditions of the surrounding atmosphere, the vertical extent of the contrail and the survival rate of ice crystals. The parameterization estimates (1) the maximum vertical displacement of the vortices in the atmosphere, (2) the vertical extent of the contrail which is given by the maximum vertical displacement of the vortices if ice crystals survive at the location of maximum displacement and smaller otherwise and (3) the survival fraction of the contrail ice crystals caused by the change in the relative humidity connected with adiabatic warming of air due to vortex descent. The parameterization captures the dependence of the survival rate on ice supersaturation, temperature, contrail ice crystal sizes and atmospheric stability. We use the parameterization assuming aircraft properties of medium sized aircraft (Aircraft type A350 or B767) (Unterstrasser, 2016 table 1) to estimate the survival rate of ice crystals and the vertical extent of the contrail after vortex descend. The contrail cross sectional area is given by the contrail vertical extent times the aircraft's wing span.

Surviving ice crystals are distributed over the contrail vertical extent after the vortex phase assuming that total plume water is distributed vertically evenly. The surviving ice crystals are distributed vertically assuming that at flight level no ice crystals sublime and assuming a linear increase in ice crystal numbers.

A survival fraction of nucleated contrail ice crystals is defined as:

$$\text{Survival fraction} = \frac{\text{number of contrail ice crystal surviving vortex descent}}{\text{total number of nucleated contrail ice crystal}} \quad (4)$$

A survival fraction of one means that all ice crystals survive the vortex descent and zero means all nucleated contrail ice crystals sublime.



## 2.2.4 Sublimation of cirrus ice crystals within the contrail's vortex descent

When contrails form within cirrus the presence of cirrus ice crystals can have an impact on the loss of ice crystals within the contrail's vortex phase. Cirrus ice crystals get entrained into the plume within the jet phase and coexist there with the contrail ice crystals. When the plume gets trapped in the wake vortices and the vortices propagate downward, temperature increases and relative humidity decreases, causing contrail and cirrus ice crystals to sublime as soon as air becomes subsaturated. The sublimation of both the cirrus and the contrail ice crystals moisten the air volume of the vortex. Therefore, the sublimation of cirrus ice crystals reduces the sublimation rate of the contrail ice crystals by weakening the decrease in relative humidity within the vortex. This may lead to a reduction in the number of contrail ice crystals that sublime within the vortex phase.

Instead of calculating the temporal evolution of contrail and cirrus ice crystal sublimation during the vortex descent, we estimate the amount of cirrus ice water that sublimates in the time during which the contrail ice crystals sublime within the descending vortices. This time is either given by the length of time the vortices descend or by the time it takes to sublime all contrail ice crystals during vortex descent. Once we have roughly estimated the amount of cirrus ice water that sublimates, we calculate the impact of the sublimated cirrus ice water on contrail ice crystal sublimation in the vortex phase. We proceed in the following way: a. We estimate the cirrus ice water mass and ice crystal number that gets entrained into the plume within the contrail's jet phase. b. We roughly estimate the cirrus ice water mass that sublimates within the time that contrail ice crystals sublime which is either given by the time the vortex descends or by the time it takes to sublime all contrail ice crystals. c. We adjust the relative humidity within the vortices consistent with the sublimated cirrus ice water mass. d. We recalculate the number of contrail ice crystals that sublime and the fraction that survives the vortex descent.

Entrained cirrus ice crystals and contrail ice crystals are different in particular regarding their size and number with cirrus ice crystals being usually significantly larger and fewer than contrail ice crystals. The water mass sublimated per ice crystal in a given time interval is larger for cirrus ice crystals than for the smaller contrail ice crystals. Cirrus ice crystals sublime only partially within the time that it takes contrail ice crystals to sublime. In order to calculate how much of the cirrus ice water sublimates within the time it takes to completely sublime all contrail ice crystals, we base our estimate on the diffusional growth equation (Pruppacher and Klett, 1980; Paoli and Shariff, 2016). It describes the growth of a single ice crystal by the deposition of water vapor onto its surface and depends on the difference between the ambient vapor pressure and the saturation vapor pressure. We roughly estimate the ratio of sublimated cirrus water mass,  $M_{\text{cirrus}}$ , and sublimated contrail water mass,  $M_{\text{contrail}}$ , by assuming spherical particles and neglecting the correction of the saturation vapor pressure over ice due to differences in ice crystal curvature (Kelvin effect) and changes in the ventilation of ice crystals:

$$\frac{dM_{\text{cirrus}}}{dM_{\text{contrail}}} \simeq \frac{r_{\text{cirrus}}}{r_{\text{contrail}}} * \frac{N_{\text{cirrus}}}{N_{\text{contrail}}} \quad (5)$$

If the background cirrus had the same ice crystal size and ice crystal number concentration as the newly formed contrail then the cirrus ice water mass sublimating in a given time interval would be the same as the contrail ice water mass. Assuming that the ice water mass entrained from the natural cirrus and connected with the contrail ice crystals is the same, the typically



290 smaller number of ice crystals from the natural cirrus leads to the sublimation of less ice water mass of the natural cirrus than  
of the young contrail within the same time unit. When keeping the cirrus ice water mass fixed, a decrease in the number of ice  
crystals leads to an increase in ice crystal mass by the same amount while the increase in the ice crystal radius is proportional  
to the third root of the volume. This means that given a fixed cirrus ice water mass the impact of cirrus ice crystal sublimation  
on the survival rate of contrail ice crystals is largest when the cirrus consists of a large number of small ice crystals (equation  
5). An increase in cirrus ice crystal numbers or ice water mass while keeping the other variable constant always leads to an  
295 increase in the contrail ice crystal's survival fraction.

### 2.3 Simulations - analysis

We study contrail formation in a large variety of atmospheric states and cloud properties over Germany using ICON-LEM at  
a horizontal resolution of 625m and a vertical resolution of approx.150m. In order to sample many different atmospheric  
conditions, we prescribe air traffic within each grid box at altitudes of between 7km and 13km assuming an average fuel  
consumption of 6 kg-fuel/km which is typical for cruise conditions over Germany according to the AEDT inventory (Wilkerson  
300 et al., 2010). Soot number emissions are set to  $2.5 \times 10^{15}$  kg-fuel<sup>-1</sup> in line with Bräuer et al., (2021). We study two different  
synoptic situations, the 24<sup>th</sup> April 2013 6am and the 26<sup>th</sup> April 2013 5pm (Sect. 3.1) starting our model with output from longer  
simulations with ICON-LEM that started on the respective days at midnight (Heinze et al., 2017). The success of the model  
simulating the large-scale synoptic situation and the associated cloud fields of those days is documented in Heinze et al.,  
305 (2017). We calculate contrail ice nucleation within cirrus and the subsequent ice crystal loss in the vortex phase on the 24<sup>th</sup>  
April 6am and 26<sup>th</sup> April 2013 5pm in all cloudy grid boxes between 7km and 13km, that is within nearly 3.5 million and  
nearly 6 million model grid boxes, respectively. For the calculation of ice crystal loss in the vortex phase we assume a fixed  
Brunt-Väisälä frequency of  $0.012 \text{ s}^{-1}$  and calculate the sensitivity to the assumed stability. Assuming a fixed Brunt-Väisälä  
frequency reduces the degrees of freedom in our calculations making it easier to isolate the impact of contrail formation on  
310 cirrus properties. When exploring the sensitivity of our results to the stability we assume a Brunt-Väisälä frequency of  $0.005$   
 $\text{s}^{-1}$ . We analyze contrail formation within pre-existing cirrus using a minimum ice water content threshold of  $10^{-11} \text{ kg m}^{-3}$ .

### 3 Impact of pre-existing cirrus on young contrails properties

We study contrail formation within natural cirrus using the high-resolution ICON-LEM. We perform case studies for two  
different synoptic situations, a high-pressure system over central Europe on the 24<sup>th</sup> and a frontal passage on the 26<sup>th</sup> April  
315 2013. In section 3.1 we introduce the synoptic situation and the cirrus properties found at that time over Germany. We study  
contrail ice nucleation and the impact of the pre-existing cirrus on contrail formation and ice nucleation (Sect. 3.2) and on the  
ice crystal loss in the vortex phase (Sect. 3.3).



### 3.1 Synoptic condition

We selected two days for our analysis, the 24<sup>th</sup> April and 26<sup>th</sup> April 2013. The days were part of the HD(CP)<sup>2</sup> HOPE measurement campaign (Macke et al., 2017) that had the goal of evaluating the performance of the high-resolution ICON simulations. The synoptic situation on those two days was very different which allows us to study contrail formation within pre-existing cirrus in strongly varying synoptic settings leading to distinct cloud microphysical properties. On the 24<sup>th</sup> April a high-pressure system dominated over Germany with close to clear sky conditions in many areas and some thin cirrus. The 26<sup>th</sup> April saw a passage of a cold front over Germany moving towards the southeast connected with a conveyor belt that was supplying the upper troposphere with moist air. Cloudiness was rapidly increasing and strong frontal convection, geometrically thick clouds and precipitation could be found along the front.

The simulations for those days were part of the model evaluation performed by Heinze et al., (2017) and Stevens et al., (2020). Heinze et al., (2017) showed that the synoptic systems on those days were simulated well by ICON. The high resolution of the ICON-LEM simulations led to improvements e.g. in the vertical cloud structure and the diurnal cycle of clouds (Stevens et al., 2020). On the 24<sup>th</sup> April cloudiness in general may be overestimated in comparison with MODIS images over central Germany while cirrus clouds, for instance in the northwest of Germany, are largely missed or are too thin in the simulations. Over the middle of Germany, a large thin cirrus cloud field with low ice water content and ice crystal number concentration is simulated in an ice saturated environment and persists for several hours. The cirrus field is spatially very homogeneous. On the 26<sup>th</sup> April, ICON simulates the frontal passage realistically and shows a slight underestimation of cloud fraction, with a good agreement regarding the cloud water path (CWP) (Heinze et al., 2017). The cirrus is scattered and microphysical properties of the cirrus vary significantly. Lifting within the frontal zone ensures a continuous water vapor supply in the upper troposphere and provides ice supersaturated conditions within the relatively thick cirrus layer. The conditions are therefore favourable for contrail formation and ice crystal growth.

We have performed a CFAD (Cloud Frequency Altitude Diagram) analysis to examine the properties, in particular the ice crystal number concentration, the mean diameter of ice crystals and ice water content (IWC), of the cirrus clouds (Fig. 2). The CFAD diagram provides information about the frequency of occurrence (probability density) of the cloud properties at different atmospheric temperatures. Figure 2 shows the frequency of occurrence of ice crystal number concentration (Fig. 2 b,e), the mean diameter of ice crystals (Fig. 2 c,f) and ice water content IWC (Fig. 2 a,d) at different temperatures in the cirrus cloud field over Germany for the 24<sup>th</sup> and 26<sup>th</sup> April 2013 at 6-7 am and 5-6 pm, respectively. On the morning of the 24<sup>th</sup> April the cirrus cloud over Germany is relatively homogeneous and the probability of cloudy areas reaching ice crystal number concentrations of roughly  $10^5 \text{ m}^{-3}$  at about 220K, a typical cruise level, is 0.01%. At the same time IWC is low and only in 0.01% of the cirrus at 220K values of  $3 \cdot 10^{-3} \text{ gm}^{-3}$  are reached. On the evening of the 26<sup>th</sup> April, the distributions of ice crystal number concentration and IWC are much wider with 0.01% of cloudy areas reaching values of up to  $10^8 \text{ m}^{-3}$  and  $0.5 \text{ gm}^{-3}$  at 220K. Describing the width of the distribution by the values occurring with a probability of 0.01%, the diameter of the ice crystals varies strongly with temperature and ranges between  $20 \mu\text{m}$  and  $200 \mu\text{m}$  at temperature 210K and between  $20 \mu\text{m}$  and



400 $\mu\text{m}$  at temperature 230K on the 24<sup>th</sup> April 2013 and on the evening of the 26<sup>th</sup> April 2013 between less than 10 $\mu\text{m}$  and 200 $\mu\text{m}$  and between 15  $\mu\text{m}$  and 600 $\mu\text{m}$  at temperature 210K and 230K, respectively. The most striking difference between the cirrus properties on the two days are the large differences in ice number concentrations with extrema in ice number concentrations at 220K about 3 orders of magnitude higher on the 26<sup>th</sup> April than on the 24<sup>th</sup> April. At the same time extrema in IWC are about 1 order of magnitude larger on the 26<sup>th</sup> April and the probability of low ice crystal sizes is increased. Those high concentrations of small ice crystals on the 26<sup>th</sup> April are likely connected with homogeneous freezing events happening in the areas of high ice supersaturation caused by lifting in the conveyor belts and with the freezing of droplets lifted within convective systems along the front. The vertical line in the diameter diagram (Fig. 2c and f) is an artefact coming from the lateral boundary conditions supplied by COSMO which is run using a 1-moment microphysical scheme. When using COSMO data for the forcing fields, a diameter of 100 $\mu\text{m}$  and associated ice crystal numbers are assumed (personal communication Axel Seifert, DWD) leading to an increased probability of ice crystals sizes of 100 $\mu\text{m}$  particularly in areas close to the model edge.

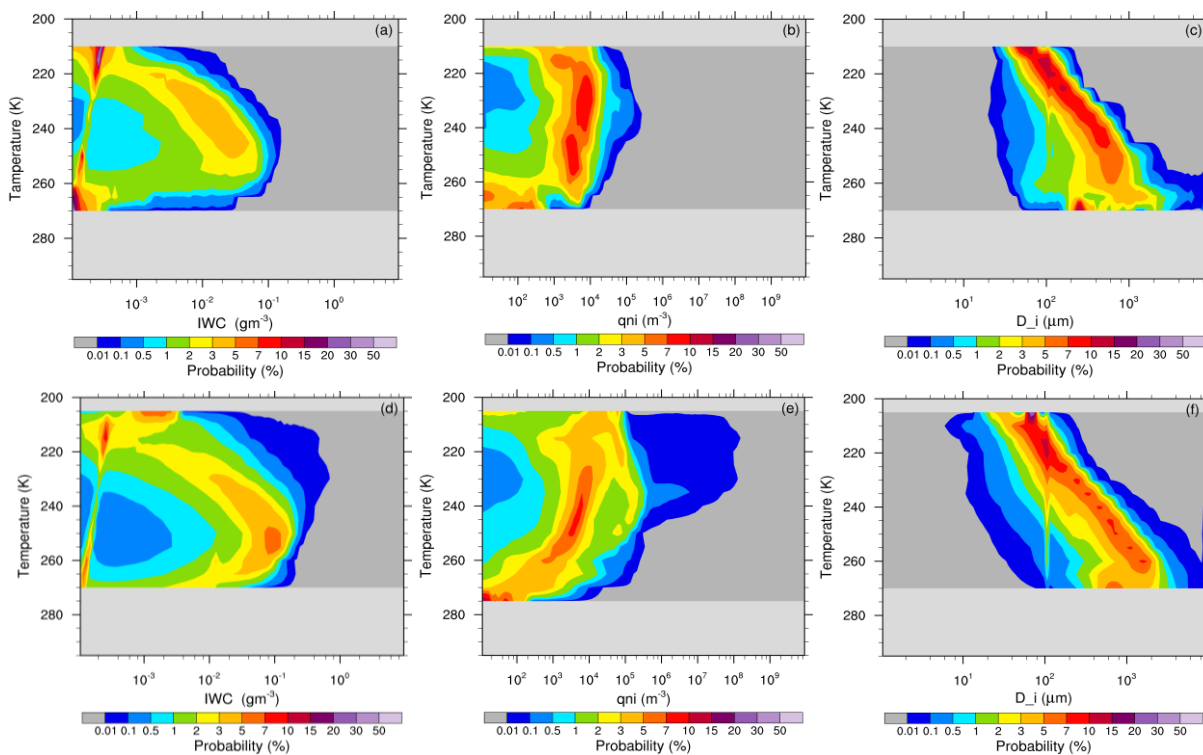


**Figure 2: Frequency of occurrence of IWC (a, d), ice crystal number concentration (b, e), and mean volume diameter of ice crystal: (c, f) on the (a,b,c) 24<sup>th</sup> April 2013 at 06 - 07 am and (d,e,f) 26<sup>th</sup> April at 5 – 6 pm. The frequencies of occurrence refer to individual temperature bins.**



### 365 3.2 Impact of the pre-existing cirrus on contrail formation and ice nucleation

We study the impact of cirrus ice sublimation on the contrail formation threshold and on ice nucleation. When aircraft fly through a cirrus cloud, air together with ice crystals get sucked through the engine inlet and sublimate. The sublimated cirrus ice crystals lead to an increase in the total water vapor in the exhaust plume. The increase is largest when the cirrus IWC is large. In the following we will call the sublimated cirrus ice crystals together with the water vapor emissions due to the combustion of fuel the ‘aviation induced increase in water vapor’. The aviation induced increase in water vapor directly affects the temperature threshold for contrail formation and the contrail ice nucleation. The probability of the ratio of cirrus ice crystal sublimation and the aviation induced increase in water vapor is generally very small. The sublimation of cirrus ice crystals usually contributes a few thousands to a few hundreds of a percent to the aviation induced increase in water vapor (Fig. 3). Maximum (probability of  $10^{-4}$ ) contributions reach values of half a percent on the 24<sup>th</sup> April 6am and 10% on the 26<sup>th</sup> April 5pm. On the 26<sup>th</sup> April contributions reach values of about 4% with a probability of  $10^{-2}$ . This is roughly in agreement with the cirrus ice water content reaching values of  $0.5 \text{ gm}^{-3}$  at 220K (Fig. 2d). Assuming a pressure of 230 hPa the ice water mass mixing ratio can be estimated and prescribing an air to fuel mixing factor of 70 kg-air/kg-fuel the cirrus ice water mass sublimated in the engine per mass of fuel burned can be shown to agree with the ratio of sublimated cirrus ice water mass and aviation induced increase in water vapor (Fig. 3).

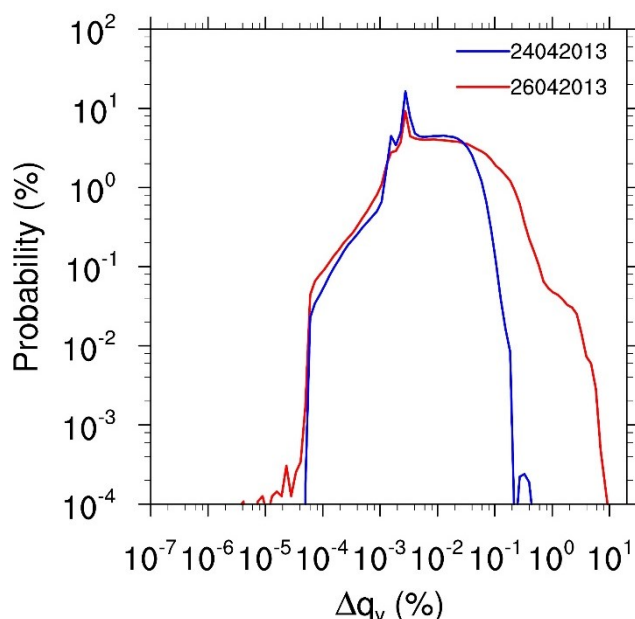


Figure 3: Probability of the ratio of cirrus ice crystal sublimation and the aviation induced increase in water vapor ‘ $\Delta q_v$ ’ due to the sublimation of cirrus ice crystals on the 24<sup>th</sup> at 6am and 26<sup>th</sup> April 2013 at 5pm for areas with temperatures lower than 233.15K, ice saturation ratio larger than 1 and IWC larger than  $10^{-11} \text{ kgm}^{-3}$ .

380



### Temperature threshold for contrail formation

Even though the sublimation of cirrus ice crystals has only a small impact on the aviation induced water vapor increase, it can result in a significant change of the Schmidt-Appleman threshold temperature,  $T_{sa}$ , (Fig. 4 c,e). On the main flight levels between 10.3 km and 10.8 km, temperatures are usually between 4 K and 10 K and between 1.5 K and 7 K lower than the contrail formation threshold (Fig. 4 a,b) on the 26<sup>th</sup> and 24<sup>th</sup> April 2013, respectively. At height levels between 9.6 km and 9.8 km i.e. at a pressure of around 270 to 280 hPa, temperatures lie mostly up to 4 K on the 26<sup>th</sup> April and up to 5 K on the 24<sup>th</sup> April below the Schmidt-Appleman threshold temperature. The change in  $T_{sa}$  on the 24<sup>th</sup> is always very low ( $< 0.1$  K) (Fig. 4e) consistent with the small impact of cirrus ice sublimation on the aviation induced water vapor increase (Fig. 3). On the 26<sup>th</sup> April, the change in the threshold temperature is often very low but changes in  $T_{sa}$  can exceed values of 0.5 K in the lower and warmer atmospheric levels (between 9.6 km and 9.8 km at ambient temperatures between 223 K and 227 K) (Fig. 4d) and values of up to 0.33 K higher in the atmosphere (between 10.3 km and 10.8 km at ambient temperatures between 215 K and 221 K) (Fig. 4c). The impact of the sublimation of cirrus ice crystals on the threshold temperature is larger at lower altitudes as the cirrus ice water content is larger at those levels (Fig. 2d) and the sublimation of cirrus ice crystals results in a larger change of the slope of the plume mixing line. On the 26<sup>th</sup> April, large changes in the contrail formation threshold temperature are associated with low ambient relative humidity (Fig. 4 c,d). An ice saturation ratio of 1 within a cirrus cloud is often indicative of a large ice crystal density that leads to an efficient relaxation of relative humidity to the saturation value. As will be shown in the next subsection, the areas of large ice crystal number concentration are on the 26<sup>th</sup> connected with ice saturation and with large IWC, the sublimation of which causes the large changes to  $T_{sa}$ . The high saturation ratios i.e. at ice saturation ratios of 1.4 and 1.5, on the other hand, indicate low ice crystal concentrations and ice water content and are likely to be the areas in which homogeneous and/or heterogeneous nucleation may occur within the next few time steps. In areas of high ice saturation ratio ( $\sim 1.4$ ) the change in  $T_{sa}$  is negligible. In the following we will explore the reasons for large changes in  $T_{sa}$  in more detail.



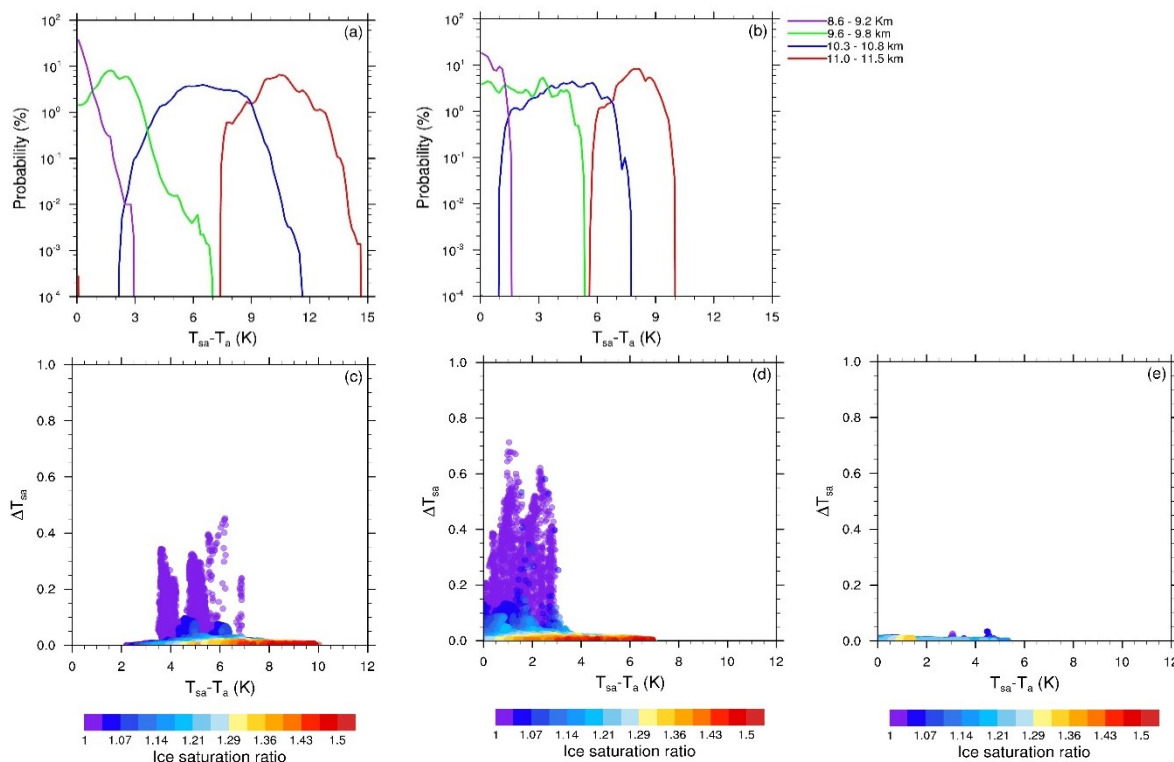


**Figure 4:** Probability distribution of difference between the Schmidt-Appleman temperature threshold of contrail formation ( $T_{sa}$ ) and the ambient temperature ( $T_a$ ) at 11 – 11.5 km (red), 10.3 – 10.8 km (blue), 9.6 – 9.8 km (green) and 8.6 – 9.2 km (purple) on the 26<sup>th</sup> April (a) and 24<sup>th</sup> April (b). Difference between the Schmidt-Appleman temperature threshold ( $T_{sa}$ ) and the ambient temperature and change in  $T_{sa}$  due to sublimation of cirrus ice crystals on the 26<sup>th</sup> April 2013 5pm at altitudes of 10.3 (~250 hPa) to 10.8km (~225 hPa) (c) and at 9.6 (~280 hPa) to 9.8km (~270 hPa) (d) and on 24<sup>th</sup> April 2013 6am at altitudes of 9.6 (~280 hPa) to 9.8km (~270 hPa) (e). In all figures the difference of ambient air temperature and  $T_{sa}$  refers to the  $T_{sa}$  that is not modified due to the sublimation of pre-existing cirrus ice.

405

### Contrail ice nucleation

Large differences between the ambient temperature and the temperature threshold for contrail formation lead to high contrail ice nucleation rates (Fig. 1). Contrail ice nucleation within pre-existing cirrus leads to large perturbations in the ice crystal number concentration of the cirrus cloud field. On the 24<sup>th</sup> April 2013 cirrus ice crystal number concentrations at 220K reach values of about  $10^5 \text{ m}^{-3}$  at a probability of 0.01% (Fig. 2b) while contrail ice nucleation leads to ice crystal number concentrations of between  $10^7$ – $10^8 \text{ m}^{-3}$  (Fig. 5b). On the 26<sup>th</sup> April 2013 the frontal system and the associated large moisture transport into the upper troposphere leads to localized nucleation events so that cirrus ice crystal number concentrations of up to  $10^8 \text{ m}^{-3}$ , the same order of magnitude as the contrail perturbations (Fig. 5a), occur with a probability of 0.01% (Fig. 2e). This means that contrail ice nucleation introduces a significant perturbation to cirrus cloud properties. Even if contrail formation is happening close to the temperature formation threshold contrail formation can significantly alter cirrus properties.

415



Close to the contrail formation threshold the number of ice crystals increases steeply with increasing distance from the threshold conditions (Fig. 1). This means that even though changes in the temperature threshold for contrail formation are moderate (Fig. 4), amounting to only several tenth of a degree, they can have a significant impact on contrail ice nucleation when the ambient temperature is close to the temperature threshold for contrail formation and when the cirrus IWC is large. Above 11 km ambient temperatures are always more than 5K below the contrail formation threshold (Fig. 4a, b) so that a change in the formation threshold would have little impact. At typical cruise levels between 10.3 km and 10.8 km the ambient temperature lies often well below the contrail formation threshold but is occasionally close to the threshold. Due to the smaller difference between ambient temperatures and the contrail formation threshold temperature, fewer ice crystals nucleate (Fig. 1; Fig. 5e, h; Fig. 6e, h). If all emitted soot particles would form an ice crystal then the grid mean ice crystal number concentration would reach approximately  $1.5 \cdot 10^8 \text{ m}^{-3}$ . At typical cruise levels contrail ice nucleation leads commonly to grid box mean ice crystal concentrations of  $1.2 \cdot 10^8$  and  $1.3 \cdot 10^8 \text{ m}^{-3}$  on the 24<sup>th</sup> (Fig. 5b) and 26<sup>th</sup> of April 2013 (Fig. 5a), respectively, but on the 24<sup>th</sup> significantly lower nucleation rates are also fairly typical. At around 9.7 km height contrail ice nucleation leads to much lower concentrations, that lie typically between  $4.0 \cdot 10^7$  and  $1.1 \cdot 10^8 \text{ m}^{-3}$  on the 26<sup>th</sup> April (Fig. 6a) and between close to 0 and  $1.3 \cdot 10^8 \text{ m}^{-3}$  on the 24<sup>th</sup> April (Fig. 6b). Contrail formation close to the formation threshold combined with large IWC of the pre-existing cirrus leads to large changes in contrail ice nucleation (Fig. 5c, e and 6c, e). On the main cruise levels, considering the sublimation of cirrus ice within the engine leads to changes in grid mean contrail ice nucleation of between  $10^2$  to  $10^6$  and  $10^5 \text{ m}^{-3}$  on the 26<sup>th</sup> April and 24<sup>th</sup> April, respectively, with changes of  $10^4$  to  $10^5 \text{ m}^{-3}$  most probable. At around 9.7 km the maximum changes are approximately one order of magnitude and by a factor of 3 larger than on the main cruise level on 26<sup>th</sup> April and 24<sup>th</sup> April, respectively. This means that on the 26<sup>th</sup> April the change in contrail ice nucleation due to the sublimation of cirrus ice crystals has the same order of magnitude as the contrail ice nucleation when neglecting the impact of sublimating cirrus ice crystals. On the 24<sup>th</sup> April the change due to the sublimation of cirrus ice crystals remains significantly lower. Absolute changes in contrail ice nucleation may be relatively small when compared to contrails that form further away from the formation threshold but they are high when compared to naturally formed cirrus clouds. Therefore, contrail ice nucleation and the changes introduced by the sublimation of cirrus ice crystals have a significant impact on cirrus properties. On the 26<sup>th</sup> of April 2013 the large IWC in the cirrus (Fig. 5c and 6c) is connected with a high number concentration of cirrus ice crystals (Fig. 5d and 6d) and with low ice saturation ratios (Fig. 5f and 6f). Large scale lifting appears to lead to the freezing of water droplets and to homogeneous nucleation events. The resulting large ice crystal number concentrations lead to an efficient relaxation of ice supersaturation to saturation values. In areas of lower ice crystal number concentrations, ice supersaturation can be large (Fig. 5 d, f and 6 d, f). The larger ice saturation ratio in those areas leads to high contrail ice nucleation rates and low corrections of this nucleation rate due to the sublimation of cirrus ice crystals in the engine. On the 24<sup>th</sup> April 2013, contrail ice nucleation is lower due to the higher temperatures (Fig. 5h) and the change in ice nucleation is lower due to the cirrus clouds containing less ice water (Fig. 5g).

At lower altitudes, between 9.6 km and 9.8 km the ambient temperature lies mostly within 5K of the contrail formation threshold (Fig. 4 a, b). At those altitudes, absolute and relative changes in contrail ice nucleation due to the sublimation of



455 cirrus ice crystals within the engine are significantly larger (Fig. 6) because the atmosphere is generally closer to the contrail formation threshold and IWC is on average slightly higher. In the upper levels we found relative changes to amount to approximately 1% while in the lower levels at around 9.7 km (Fig. 6) the relative change can amount to 200% of the ice nucleation when neglecting the impact of cirrus ice crystals when temperatures are very close to the formation threshold. At both altitude ranges, maximum absolute changes in ice nucleation are between 1 and 2 orders of magnitude smaller on the 24<sup>th</sup> April than on the 26<sup>th</sup> April 2013 owing to the lower IWC (Fig. 5g, 6g) and ice saturation ratio (not shown).

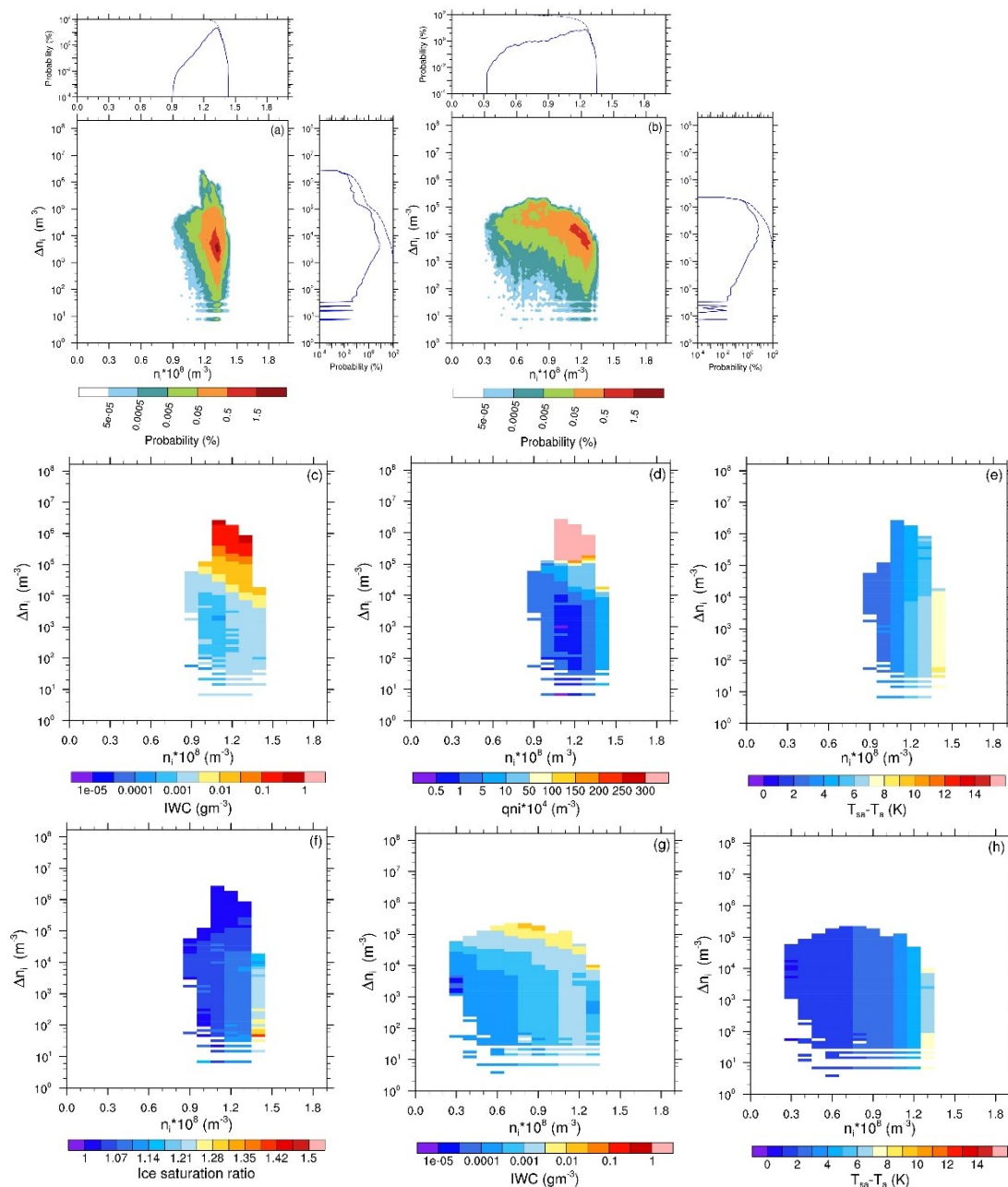


**Figure 5: Joint probability distribution of grid mean ice crystal number concentration due to contrail ice nucleation,  $n_i$ , and its change due to the sublimation of cirrus ice crystals within the aircraft engine,  $\Delta n_i$ , for current soot number emissions,  $2.5 \cdot 10^{15}$  kg-fuel<sup>-1</sup> and for altitudes from 10.3km to 10.8km (250 hPa to 225 hPa) on the (a) 26<sup>th</sup> April and (b) 24<sup>th</sup> April 2013. Additionally, the PDF of ice nucleation (solid) and the associated cumulative PDF (dashed) when neglecting the impact of natural cirrus ice crystals (top) and its change due to the sublimation of cirrus ice crystals (right) is shown. Mean ice cloud properties for the combination of  $n_i$  and  $\Delta n_i$  (c,g) IWC, (d) qni, (e, g) difference between temperature formation threshold and ambient temperature and (f) SSL. (c), (d), (e) and (f) for cirrus cloud properties on the 26<sup>th</sup> April 2013 6am and (g) and (h) for the 24<sup>th</sup> April 2013 5pm. If all emitted soot particles would form an ice crystal then the ice crystal number concentration within the grid box,  $n_i$ , would reach approximately  $1.5 \cdot 10^8$  m<sup>-3</sup>.**

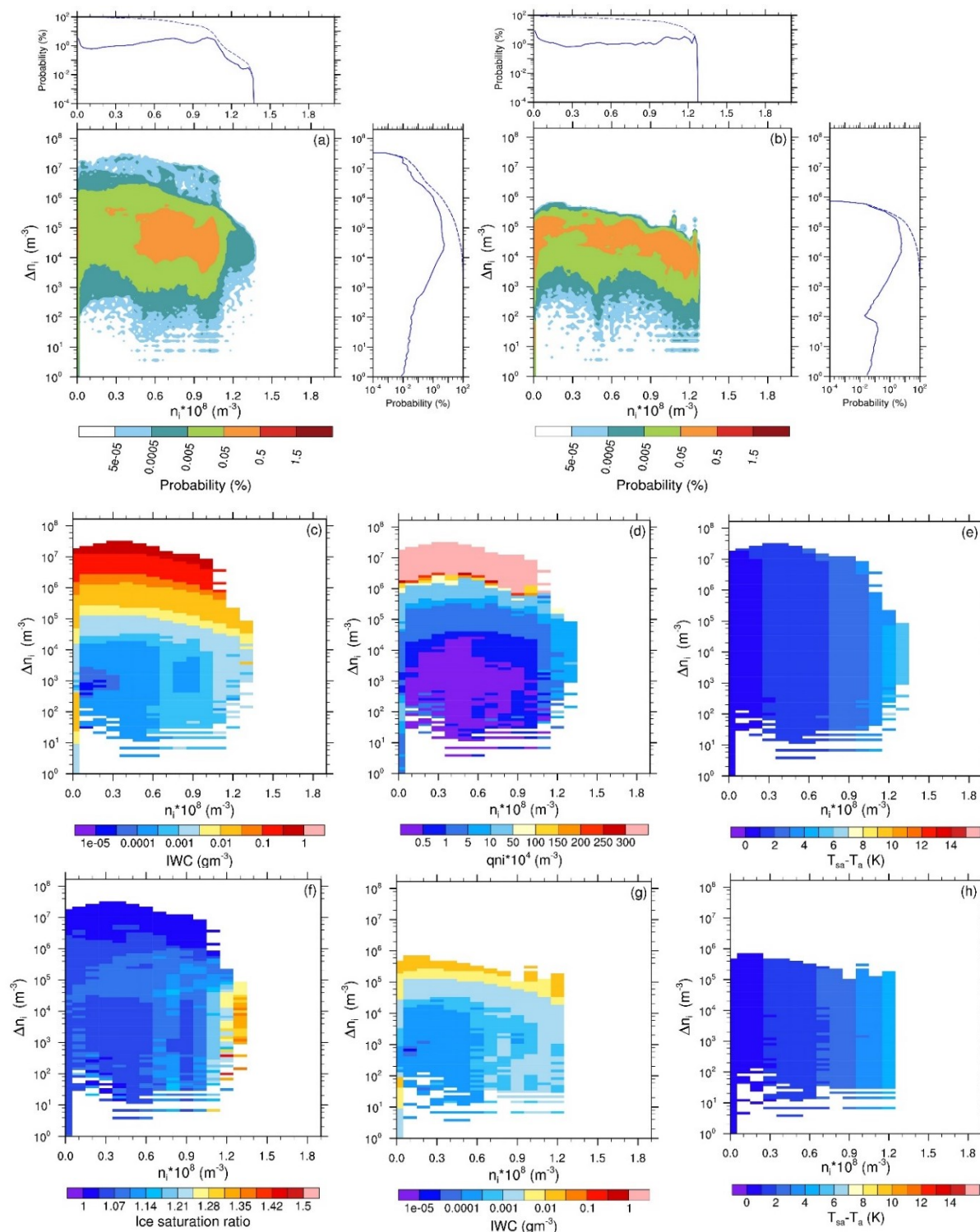


Figure 6: As figure 5 but for altitudes ranging from 9.6km (280 hPa) to 9.8 km (270 hPa).



### 3.3 Impact of the pre-existing cirrus on ice crystal loss during the vortex phase

460 Here we analyze the ice crystal loss during the vortex phase and the impact of pre-existing cirrus ice crystals that get mixed  
into the plume before the vortex phase on the ice crystal loss. The sublimation of cirrus ice crystals can increase the survival  
rate of contrail ice crystals during the vortex phase since cirrus ice crystals, that are mixed into the plume during the contrail's  
jet phase, sublimate together with the contrail ice crystals increasing the relative humidity slightly. This increase in relative  
humidity within the vortices relative to vortices that do not contain natural cirrus ice crystals can lead to a decrease in the ice  
465 crystal loss and therefore an increase in the ice crystal survival rate.

We have analyzed the impact of cirrus ice crystals on the survival of contrail ice crystals during the contrail's vortex phase  
separately for contrails that form more than 5K below the temperature threshold for contrail formation (Fig. 7) and for contrails  
that form closer to the formation threshold (Fig. 8). For contrails forming more than 5K below the temperature threshold we  
assume that the number of nucleated ice crystals can be approximated by the emitted soot number (Kärcher et al., 2015). That  
470 means that we assume that the  $AEI_i = EI_s$ , that is  $2.5 \cdot 10^{15} \text{ kg-fuel}^{-1}$ , for current day soot number emissions. For contrails forming  
closer than 5K below the contrail formation threshold we calculate first ice crystal nucleation according to the parameterization  
of Kärcher et al., (2015) and then calculate the survival fraction which is dependent on the number of nucleated ice crystals.  
In both cases we assume an atmospheric stability of  $0.012 \text{ s}^{-1}$ , a value that is slightly higher than the average in the upper  
troposphere, and examine the sensitivity to that assumption.

#### 475 3.3.1 Far-below-threshold case

On the 24th of April 2013, it is mainly the atmospheric levels above 11 km and a few hundred meters below where the  
temperature is more than 5K below the contrail formation threshold (Fig. 4b). At those levels the fraction of ice crystals  
surviving the vortex phase, when neglecting the impact of natural cirrus ice crystals, and its change caused by the sublimation  
of natural cirrus ice crystals within the vortex are both very small (Fig. 7a). Only in about 1% of grid boxes survival fractions  
480 of about 0.35 are exceeded. Reasons for that are the low ice supersaturation and IWC within the very thin cirrus (Fig. 2) causing  
a low total water (water vapor plus condensate) content within the aircraft plume. The change in the survival fraction is very  
low because of the low IWC in the pre-existing cirrus (Fig. 2) leading to a maximum change in the aviation induced water  
vapor content of the plume of 0.5% only (Fig. 3). At very low survival rates (below about 0.2), its change due to cirrus ice  
crystal sublimation can amount to up to 0.05% but overall the effect can be neglected.

485 On the 26<sup>th</sup> April, the temperature on the atmospheric levels above about 10 km is more than 5K below the contrail formation  
threshold (Fig. 4a). At those levels ice supersaturation and cirrus ice water content (Fig. 2) are significantly larger than on the  
24<sup>th</sup> April due to the large-scale rising motion connected with the frontal system. Therefore, ice crystal survival fractions and  
in particular their change due to the impact of cirrus ice crystals are larger (Fig. 7b). When sampling all grid boxes that have  
temperatures more than 5K below the contrail formation threshold, the probability of low survival fractions of up to 10% is  
490 highest but survival fractions of up to 90% can be found. In about 1% of grid boxes survival fractions exceed 40%. The impact





of cirrus ice crystals on the survival fractions is low, reaching maximum values of up to 3-4% only. In about 0.01% of the grid boxes changes in the survival fractions amount to 2% or more. The highest changes to the ice crystal survival fraction are found in situations when the ice crystal survival is low. This means that the change in the survival fraction due to the impact of the natural cirrus ice crystals is not negligible in areas with low survival fractions. When survival fractions lie between 40-495 50% the change in the survival fraction can reach values of around 1% only. In fewer than 1% of the grid boxes the change in the survival fraction amounts to half a percent. In the following we study the dependency of the survival fraction and its change due to the sublimation of natural cirrus ice crystals on the various parameters discussed in Sect. 2.

### Sensitivity to soot number emissions and static stability

500 A reduction in soot number emissions leads to fewer ice crystals nucleating within the aircraft plume (Kärcher et al., 2015). A smaller number of contrail ice crystals within a plume with unchanged total water content leads to a larger fraction of contrail ice crystals surviving the vortex descent (Fig. 7c,d; Unterstrasser, 2016). This explains the increased probability of high survival fractions and the decreased probability of low survival fractions and the slight increase in the maximum survival fraction for the decrease in soot number emissions by 50% (Fig. 7c) and by 80% (Fig. 7d). In 1% of grid boxes survival fractions exceed 70% and in 10% of grid boxes survival fractions exceed 30% at 80% reduced soot number emissions. 505 Furthermore, the decrease in the soot number emissions affects the change in the survival fraction due to the sublimation of natural cirrus ice crystals. The decrease in soot number emissions leads to an increase in the contrail ice crystal sizes, with the relative increase in sizes smaller than the relative decrease in numbers. Therefore, a larger part of the ice water content of the natural cirrus can sublimate in the time it takes the contrail ice crystals to sublimate during vortex descent (equation 3). This leads to a larger increase in the relative humidity within the descending vortex and consequentially to an increase in the contrail ice crystal survival fraction. While for normal soot number emissions a change in the ice crystal survival fraction of 1% at a survival fraction of 40-50% is not uncommon on the 26<sup>th</sup> April 2013, this change in the survival fraction is increased to 1.5% and 2% for soot number emissions reduced by 50% (Fig. 7c) and 80% (Fig. 7d), respectively. In about 0.005% (that is in nearly 1000 cloudy grid boxes) and 0.02% of the grid boxes changes in the survival fraction exceed 7% for 50% and 80% reduced soot number emissions, respectively. The probability of finding larger survival fraction changes than 3% is ~0.003%, 0.03% and 0.1% of grid boxes for current day soot number emissions and for reductions of 50% or 80%, respectively. 515

The atmospheric stability determines the maximum vertical displacement of the wake vortices with high stability limiting the descent of the vortex. A low stability leads to a large descent of the vortex and therefore to a large decrease in relative humidity within the vortex and a decreased ice crystal survival fraction. We have analyzed the effect of atmospheric stability on the survival rate of contrail ice crystals by lowering the upper tropospheric Brunt-Väisälä frequency to a value of  $0.005\text{s}^{-1}$  (Fig. 7c). A larger fraction of the contrail ice crystals sublimate during vortex descent in a weakly stable atmosphere (Unterstrasser, 2016, Fig. 7c). The probability of high survival fractions of contrail ice crystals decreases and the probability of large changes in the survival fraction due to the presence of natural cirrus ice crystals decreases. In particular the probability of large changes in the survival fraction at survival fractions of close to zero is significantly reduced in a weakly stable atmosphere. 520



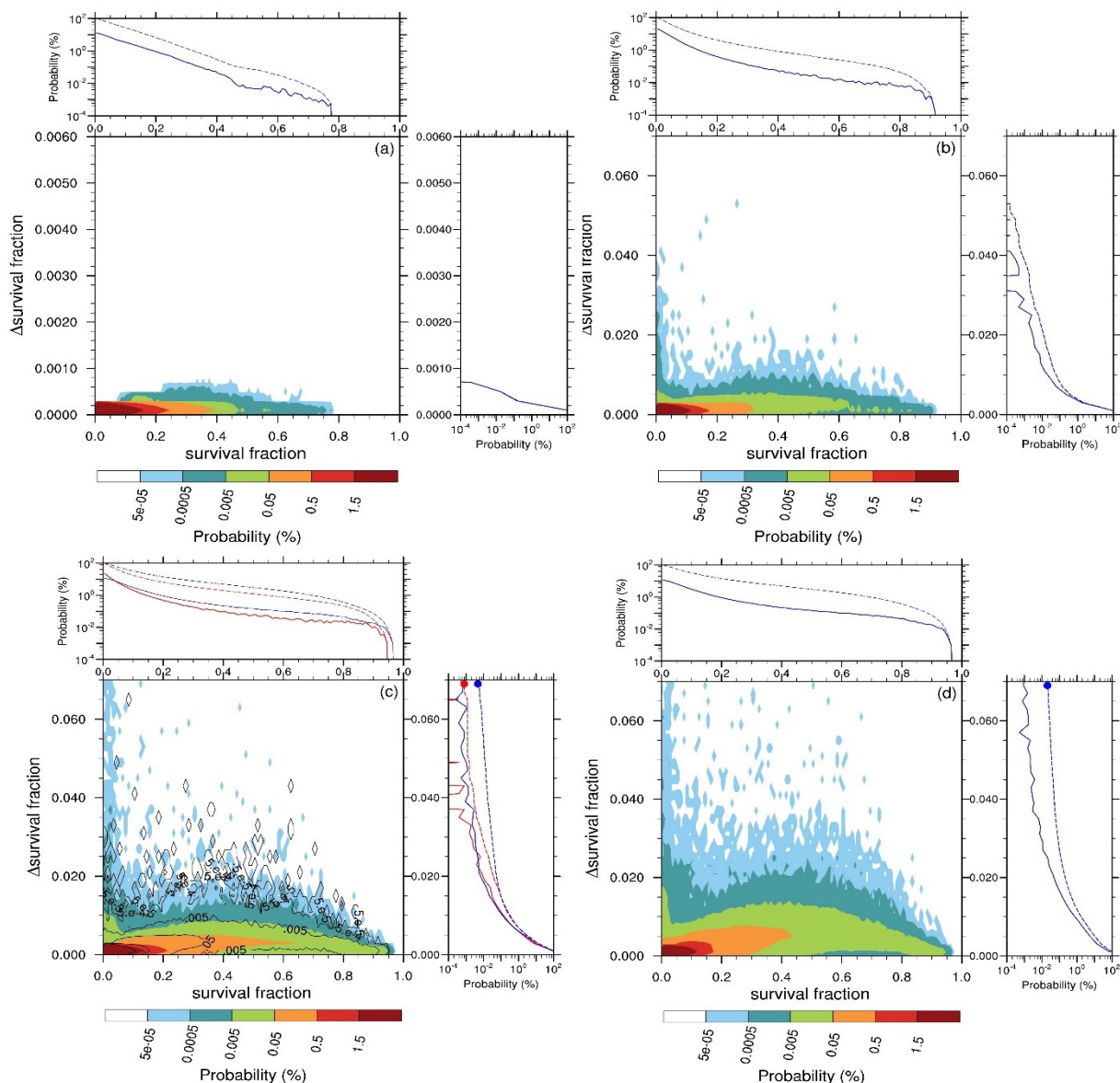


**Figure 7: Joint probability distribution of contrail ice crystal survival fraction during the vortex phase when neglecting the impact of cirrus ice crystals and its change due to the sublimation of cirrus ice crystals for current soot number emissions,  $2.5 \times 10^{15}$  kg-fuel<sup>-1</sup>, for (a) the 24<sup>th</sup> April and (b) the 26<sup>th</sup> April 2013 and for the 26<sup>th</sup> April for (c) 50% reduced soot number emissions and (d) 80% reduced soot number emissions. Additionally, the PDF of the fraction of surviving ice crystals (solid) and the associated cumulative PDF (dashed) when neglecting the impact of natural cirrus ice crystals (top) and its change due to the presence of cirrus ice crystals (right) is shown. A Brunt-Väisälä frequency of  $0.012 \text{ s}^{-1}$  (strong stability) has been assumed for all cases. In (c) red lines indicate the probabilities when reducing the Brunt-Väisälä frequency to  $0.005 \text{ s}^{-1}$  (weak stability). Note that in (a) the scale of the y-axis is changed compared to the other figures. Ice crystal survival fractions were calculated whenever the ambient temperature was 5K below the temperature threshold for contrail formation. The dots in the probability distribution of the change in survival rate (right) indicate the probability of changes in the survival fraction that are larger than 7%. Delta survival fraction is defined as the difference between the survival fraction when considering cirrus ice crystal sublimation minus when neglecting the impact of cirrus ice crystals on the survival fraction.**



### Impact of cirrus cloud properties

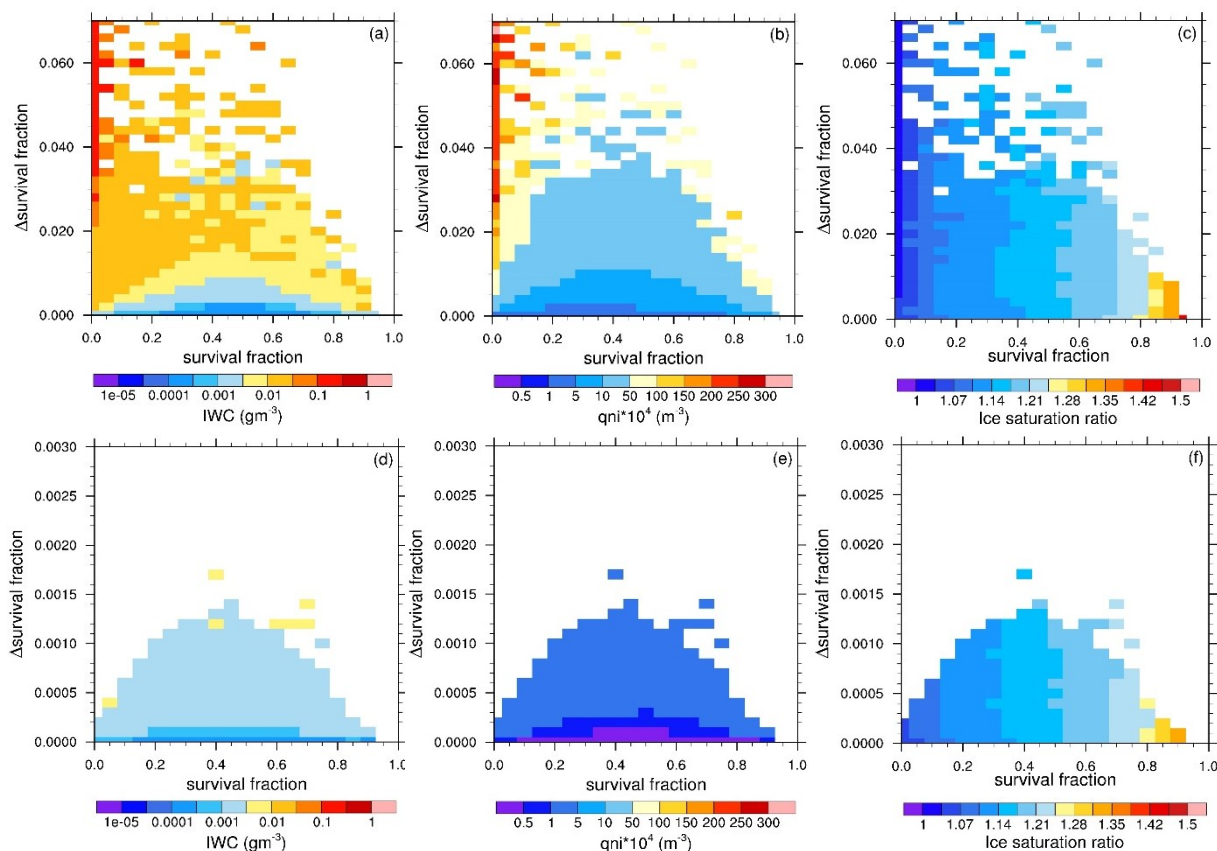
The strength of the impact of the sublimating natural cirrus ice crystals on the fraction of contrail ice crystals surviving the vortex phase depends not only on the number of contrail ice crystals forming and on the atmospheric static stability but also on the cirrus properties, in particular the cirrus ice crystal number concentration and ice crystal sizes (equation 3), and on the development of relative humidity within the plume due to the descent. The higher the ice crystal number concentration and the ice crystal radii within the cirrus the more cirrus ice mass can sublime and the stronger the impact of the pre-existing cirrus on the contrail ice crystal survival fraction.

Fig. 8 shows the cirrus properties, IWC, ice crystal number concentration and in-cloud ice supersaturation, for each set of survival rate of contrail ice crystals and its change due to the sublimation of natural cirrus ice crystals for the 26<sup>th</sup> April and the 24<sup>th</sup> April case. A soot number emission of  $0.5 \cdot 10^{15} \text{ kg-fuel}^{-1}$  and a Brunt Väisälä frequency of  $0.012 \text{ s}^{-1}$  has been prescribed. As expected (see Sect. 2.2.3 for the discussion of the importance of ice supersaturation for contrail formation in cloud-free air), the in-cloud saturation ratio with respect to ice affects the survival rate of the contrail ice crystals with high ice supersaturation leading to high contrail ice crystal survival rates (Fig. 8c, f). If ambient air is close to saturated with respect to ice (saturation ratio close to 1.0) then the adiabatic warming in the descending vortices will lead to strong sub-saturations so that survival fractions are very low and mainly only the ice crystals within the secondary vortex can survive. On the 26<sup>th</sup> April, the pre-existing cirrus has a large impact on the survival of contrail ice crystals within the vortex phase if the cirrus ice water content and the ice crystal number concentrations are high (Sect. 2.2.4; Fig. 8 a,b). Large cirrus ice crystal number concentrations are commonly connected with relative humidity around ice saturation. Therefore, areas with high cirrus ice crystal number concentrations are often areas where the contrail ice crystal survival rate (when neglecting the impact of cirrus ice crystals) is low (Fig. 8b) and when they are connected with relatively high IWC (Fig. 8a, b), the pre-existing cirrus has a relatively large impact on the contrail ice crystal survival rate. Survival rates of more than 50%, when neglecting the impact of cirrus ice, are usually connected with ice saturation ratios above around 1.2. In those areas high cirrus ice crystal numbers are relatively uncommon and hint at recent ice nucleation events presumably connected with the fast lifting of moist environmental air within the frontal system. In areas where the survival fraction is larger than 50%, high ice number concentrations and IWC lead only occasionally to changes in the survival fraction of more than 2%-3%. At lower survival fractions, large cirrus ice crystal number concentrations and IWC can lead to large absolute and relative changes in the contrail ice crystal survival fractions. For example, for the 26<sup>th</sup> April case in about 85% of grid boxes the survival rate (without considering the impact of sublimating cirrus ice crystals) is below 0.2. For those grid boxes the relative change in the survival fraction can be 20%. That means that delta survival fraction can be as large as 0.04 for a survival fraction (without considering the impact of sublimating cirrus ice crystals) of 0.2.

On the 24<sup>th</sup> April IWC and in particular ice crystal number concentrations (Fig. 8d and e) are much smaller than on the 26<sup>th</sup> April leading to much lower changes in the survival rate due to the sublimation of cirrus ice crystals (Fig. 7a). Cloud areas that



560 have a comparable IWC on the two days, still have lower ice crystal number concentrations on the 24<sup>th</sup> leading to smaller changes in the ice crystal survival rate on the 24<sup>th</sup> April 2013.



**Figure 8:** Ice cloud properties for combinations of contrail ice crystal survival fraction during the vortex phase when neglecting the impact of cirrus ice crystals and its change due to the sublimation of cirrus ice crystals, delta survival fraction, for the 26th April (a, b, c) and for the 24th April (d, e, f) for cases of contrail formation more than 5K below the contrail formation threshold. Color coded are the cloud properties of the preexisting cirrus, IWC (a, d), cirrus ice crystal number concentration (b, e) and in-cloud ice saturation ratio (excluding emission and sublimation of ice) (c, f). A Brunt-Väisälä frequency of  $0.012\text{s}^{-1}$  and soot number emissions of  $0.5 \cdot 10^{15} \text{kg-fuel}^{-1}$  are assumed. Note that the scale on the y-axis is changed in figures for the 24<sup>th</sup> April 2013.

### 3.3.2 Close-to-threshold case

565 Prescribing soot number emissions of  $0.5 \cdot 10^{15} \text{kg-fuel}^{-1}$ , the probability density function of survival fractions of ice crystals forming close to the contrail formation threshold (Fig. 9) is similar to the one for the far-from-threshold cases (Fig. 7d) when neglecting the impact of cirrus ice crystals. Large survival fractions are slightly less common in the close-to-threshold cases. In the grid boxes where temperatures are close to the formation threshold, about 1% (10%) of the grid boxes survival fractions are larger than 65% (25%) whereas in the far-from-threshold cases the same percentage of grid boxes exceeds survival fractions of 70% (30%).



570 The probability of changes in the survival fraction, due to the sublimation of cirrus ice crystals, exceeding 1% is significantly smaller in the close to formation threshold cases. But maximum changes in the survival fraction are much larger when contrails form close to the contrail formation threshold. In 0.1% of cases the change in the survival fraction exceeds 4% but changes can also reach occasionally values of 20% and higher.

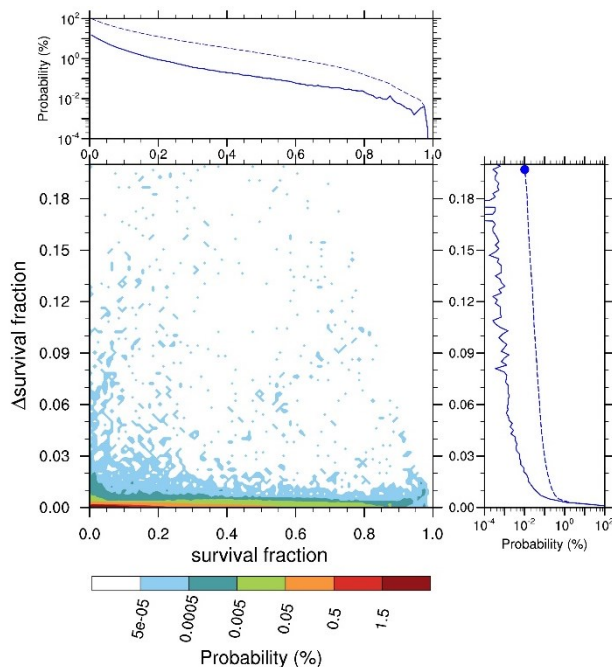


**Figure 9:** Joint probability distribution of contrail ice crystal survival fraction during the vortex phase when neglecting the impact of cirrus ice crystals and its change due to the sublimation of cirrus ice crystals for the 26th April 2013 when contrails form closer than 5K from the contrail formation threshold. Additionally, the PDF of the fraction of surviving ice crystals (solid) and the associated cumulative PDF (dashed) when neglecting the impact of natural cirrus ice crystals (top) and its change due to the presence of cirrus ice crystals (right) is shown. A Brunt-Väisälä frequency of  $0.012 \text{ s}^{-1}$  (strong stability) and soot number emissions of  $0.5 \cdot 10^{15} \text{ kg-fuel}^{-1}$  have been prescribed. The dots in the probability distribution of the change in survival rate (right) indicate the probability of a change in the survival fraction that is larger than 20%. Bin size is 0.002.

575 Studying the reasons for the change in the survival fraction of contrail ice crystals due to cirrus ice crystal sublimation when contrails form close to the contrail formation threshold is complicated by the fact that the survival is additionally dependent on the number of nucleated contrail ice crystals which varies depending on the atmospheric state. Assuming fixed soot number emissions, the ambient atmospheric state controls contrail ice nucleation while the survival of the ice crystals during the vortex phase is dependent on atmospheric variables and on the contrail ice nucleation.

580 High survival fractions are found in areas where either the in-cloud ice saturation ratio is high or where contrail formation occurs close to the formation threshold so that the number of nucleated contrail ice crystals is very low and ice supersaturation ratios are average. Due to the low number of contrail ice crystals, the ice crystals are larger and the survival fraction within the vortex phase is increased, similar to the increased survival fractions when reducing soot number emissions. The fact that



survival rates can be high either when the ice supersaturation ratio is high or when it is average but very few contrail ice crystals formed hide the strong influence ice supersaturation has on the survival of ice crystals (Fig. 10c).

585 The change in the survival fraction is primarily a function of how close to the formation threshold contrails were formed and, therefore, of the  $AEI_i$ . The closer contrail formation happens to the threshold the fewer ice crystals are formed, so that the impact of the pre-existing cirrus on the survival fraction can be relatively large (Fig. 10d, e). Large changes are also found for high  $AEI_i$  when cirrus IWC and ice crystal number concentrations are particularly large (Fig. 10a, b). Changes in the survival fraction larger than 5% are only found if  $AEI_i$  is 2 orders of magnitude or more below the soot number emission index or when

590 the survival fraction (when neglecting the impact of cirrus ice crystal sublimation) is close to zero (below about 2%). In cases when very few ice crystals form in the contrail, the correction in the survival fraction is large despite low cirrus ice crystal number concentrations and average IWC. In those situations, it is few but large cirrus ice crystals that partly sublimate that increase the survival fraction of contrail ice crystals significantly. In cases where the IWC and cirrus ice crystal number concentration is high, many contrail ice crystals nucleated despite low ice supersaturation ratios. In those cases the survival

595 fraction, when neglecting the impact of cirrus ice sublimation, is very low but corrections can be very large. It is those areas where the impact of pre-existing cirrus on both contrail ice nucleation and survival is particularly large.



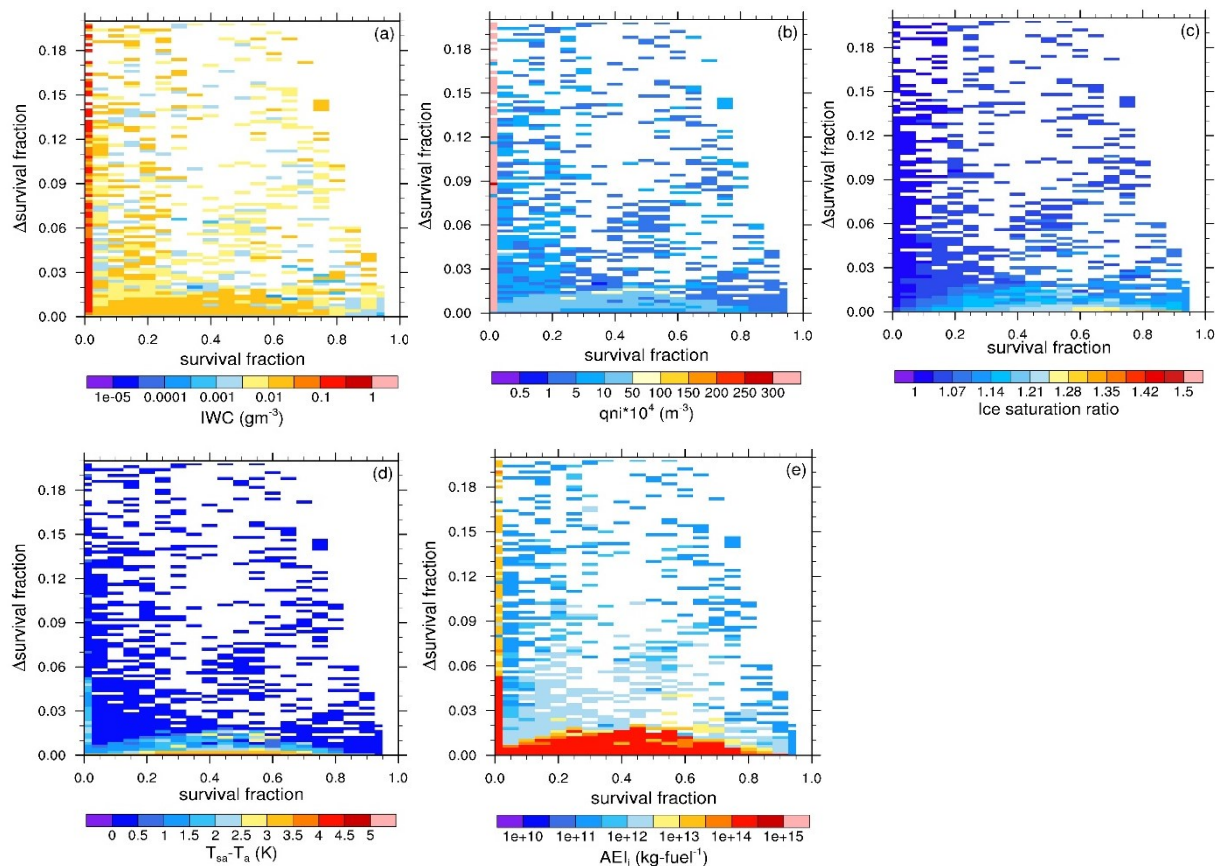


**Figure 10: Ice cloud properties for combinations of contrail ice crystal survival fraction during the vortex phase when neglecting the impact of cirrus ice crystals and its change due to the sublimation of cirrus ice crystals, delta survival fraction for the 26<sup>th</sup> April for contrail formation at temperatures closer than 5K from the contrail formation threshold. Color coded are the cloud properties of the preexisting cirrus, IWC (a), cirrus ice crystal number concentration (b), in-cloud ice saturation ratio (c), temperature distance from the ‘new’ formation threshold (d) and ‘new’ apparent emission index of contrail ice crystals (e). In figures (d) and (e) ‘new’ indicates that changes due to the sublimation of cirrus ice crystals have been considered. A Brunt-Väisälä frequency of  $0.012\text{s}^{-1}$  and soot number emissions of  $0.5 \cdot 10^{15} \text{ kg-fuel}^{-1}$  are assumed.  $AE_i$  of  $5 \cdot 10^{14}$  translates into  $qn_i = 3 \cdot 10^7 \text{ m}^{-3}$ . The correction of ice nucleation due to sublimation of cirrus ice crystals during combustion is considered.**

#### 600 4 Summary and comparison with literature

The impact of pre-existing cirrus on contrail formation, the change in the contrail formation criterion and in ice crystals survival in the vortex phase, has been discussed by Gierens (2012). In agreement with Gierens (2012) we find that the sublimation of the ice crystals that get sucked into the aircraft’s engine increase plume relative humidity only very slightly. The impact of ice crystal sublimation within the engine on the aviation induced change in humidity in the aircraft plume amounts to maximally  
 605 a few percent in case of the thick frontal cirrus and to less than 1% in the case of the very thin cirrus event. This slight increase leads to changes in the contrail formation threshold of a few tenth of a degree. In case of the frontal cirrus the contrail formation



610 criterion is changed by up to 0.7K. In large parts of the cirrus cloud field the presence of cirrus does not impact the contrail formation criterion and contrail ice nucleation significantly. In areas where the cirrus IWC is largest the contrail formation threshold temperature and contrail ice nucleation can be modified significantly. Since contrail ice nucleation is nonlinearly dependent on the difference between ambient air temperatures and the temperature threshold for contrail formation (Kärcher et al., 2015), the change in the contrail formation threshold leads to large relative changes in contrail ice nucleation at temperatures close to the formation threshold. Relative changes in contrail ice nucleation are, therefore, large at times when contrail ice nucleation is otherwise low, i.e. when contrails form close to the formation threshold. Nevertheless, a low contrail ice nucleation can still induce a large perturbation in cirrus ice crystal numbers.

615 The most important predictor for a large change in ice nucleation due to sublimated ice crystals is the cirrus IWC. A large cirrus IWC causes a large change in contrail ice nucleation which means that changes in contrail ice nucleation due to pre-existing cirrus can be particularly large in lower flight levels and in the tropics (Bier and Burkhardt, 2019) as in those areas the IWC is usually larger and contrail ice nucleation lower. At the lower flight levels, at around 9.7 km the change in the ice nucleation due to the sublimation of pre-existing cirrus ice crystals can be as large as the contrail ice nucleation calculated when neglecting the impact of the pre-existing cirrus. We, therefore, conclude that the sublimation of cirrus ice crystals in the engine can have a significant impact on contrail formation, contrary to the conclusion of Gierens (2012) who considered the impact of the sublimation of cirrus ice crystals on the contrail formation criterion but not on contrail ice nucleation. Nevertheless, we agree with Gierens (2012) that the use of alternative fuels and the associated increase in water vapor emissions by about 10% will have significant implications for ice nucleation, but we estimate that this effect can be matched by the impact of pre-existing ice crystals in very thick natural cirrus.

625 Ice crystals that are mixed into the aircraft plume before the start of the vortex phase are caught in the descending vortices together with the contrail ice crystals. In the descending vortices temperature increases and relative humidity decreases. Once relative humidity decreases below saturation both cirrus and contrail ice crystals will start to sublimate. The sublimation of cirrus ice crystals in the descending vortices causes an increase in relative humidity which leads to an increase in the time it takes the contrail ice crystals to sublimate. Since cirrus ice crystals are commonly larger than ice crystals in young contrails, cirrus ice crystals will sublimate only partly in the time it takes to sublimate contrail ice crystals completely. Nevertheless, the sublimation of cirrus ice crystals can lead to a decrease in the number of contrail ice crystals that sublimate completely and therefore to an increase in the survival fraction of contrail ice crystals. We find that for current day soot emissions ( $EI_s=2.5 \cdot 10^{15}$  kg-fuel<sup>-1</sup>) changes in the survival fraction are maximally a few percent when contrails form more than 5K below the formation threshold in a stably stratified atmosphere. Changes in the survival rate are largest in cirrus that comprise large cirrus ice crystal number concentrations and IWC. When reductions in soot number emissions are introduced, e.g. caused by the introduction of alternative fuels, contrail ice nucleation is reduced by approximately the same degree as the soot number emissions which leads to an increase in the contrail ice crystal sizes and in the survival fraction when neglecting the impact of cirrus ice crystals. The larger contrail ice crystal sizes also lead to a larger change of the survival fraction due to the sublimation of cirrus ice crystals because the difference between the contrail and cirrus ice crystal sizes gets smaller. Large changes in the survival





fraction of ice crystals are uncommon for contrail formation far below the formation threshold even for 80% reduced soot number emissions. Only in 0.1% of the cirrus volume changes in the survival rate amount to more than 3%. In an atmosphere with reduced stability both the survival rate and its change due to the sublimation of cirrus ice crystals are reduced.

When contrail formation happens close to the formation threshold, the change in the ice crystal loss caused by the sublimation of cirrus ice crystals can be significantly larger than in far-from-threshold cases, but the probability of those large changes is very low. Absolute changes in the survival rate amount maximally to about 20% in case of the frontal cirrus when assuming 80% reduced soot number emissions and a stably stratified atmosphere. Large changes in the survival rate, amounting to a few percent, are often connected with low AEI<sub>i</sub>, i.e. with low contrail ice nucleation, in an atmosphere that is only weakly ice supersaturated. In those situations, changes in the survival fraction are high even though cirrus IWC and ice crystal number concentrations are low. The change in ice crystal survival can be also large in situations when many contrail ice crystals formed in situations close to the contrail formation threshold within cirrus that comprises a large IWC and ice crystal number concentration. In case of contrail formation within very thin cirrus clouds, e.g. in 24th April 2013 case, the change in the ice crystal survival rate is insignificant.

Gierens (2012) compared the sublimation time scale of typical contrail and cirrus ice crystals. He estimated that the sublimation time scale for cirrus ice crystals was about 100 times larger than the respective time scale for contrail ice crystals assuming average cirrus properties and, therefore, concluded that the effect cannot be important. Contrary to Gierens (2012), our calculations indicate that the sublimation of contrail ice crystals can be significantly changed even if cirrus ice crystals are significantly larger. This is because the impact of cirrus ice crystal sublimation does not depend on the difference of the sublimation time scales but rather on the cirrus water mass that can be sublimated in the time it takes to sublimate contrail ice crystals. The larger the cirrus ice water content and ice crystal concentration the larger is the impact of the cirrus ice sublimation on the relative humidity within the plume and on the contrail ice crystal survival rate. Contrail formation within aged contrail cirrus would lead to even larger contrail ice crystal survival rates.

Percentages of the cirrus volume in which contrail formation is affected by pre-existing cirrus are very much dependent on the definition of a cirrus cloud. By including extremely thin cirrus in our analysis (using an IWC threshold of  $10^{-11}$  kg m<sup>-3</sup>) the fraction of the cirrus volume with high IWC, is low and therefore with a significant impact of the pre-existing cirrus, is low. Restricting our analysis to cirrus with larger IWC or larger optical depth, e.g. to only those cirrus that would be visible by eye from the ground, would lead to an increase in the likelihood with which pre-existing cirrus can have an impact on contrail formation.

## 5 Conclusions

Contrail formation constitutes a significant perturbation to cirrus cloudiness. Until now it is mainly the impact of contrail formation in cloud free air that has been studied. Recently, satellite observations of cirrus perturbations caused by contrail formation within cirrus resulting in an increase of cirrus optical depth (Tesche et al., 2016) have led to increased interest in the



topic. Here we present a contrail parameterization, consisting of the estimation of contrail formation conditions, contrail ice nucleation and contrail ice crystal loss in the vortex phase, within ICON-LEM (Zängl et al., 2015) centered over Germany. We study contrail formation within cirrus and whether contrail formation is modified due to the impact of pre-existing cirrus. It has been argued before that the presence of pre-existing cirrus ice crystals do not impact contrail formation or ice crystal survival during the vortex phase significantly (Gierens, 2012). We choose two very different synoptic situations, a high-pressure ridge and a frontal passage over Germany, sampling a large range of cirrus cloud properties to study contrail formation within cirrus. We find that ice nucleation within contrails leads to ice crystal number concentrations of approximately  $10^8 \text{ m}^{-3}$  in young contrails. Even if only 10% of those ice crystals survive the contrail's vortex phase this still often leads to a local increase of the cirrus ice crystal number concentration about 3 orders of magnitude. The pre-existing cirrus ice crystals often have a negligible impact on the contrail formation processes but in case of cirrus with a large IWC and ice crystal number concentration, such as in our frontal cirrus situation, contrail formation can be noticeably modified.

Analyzing the whole cirrus cloud field over Germany, we find that cirrus clouds have only seldomly large enough IWC and ice crystal number concentration so that they have a noticeable impact on contrail formation. Those areas are connected e.g. with the vertical transport of moist air within warm conveyor belts connected with frontal activity. This means that changes in contrail formation due to pre-existing cirrus are large in areas where cirrus disturbances are most likely to have a long-life time and, therefore, may exert a significant radiative impact. The change in cirrus ice crystal numbers due to contrail formation and the impact of pre-existing cirrus on contrail formation are both influencing cirrus optical depth, radiative fluxes and cirrus life times in those frontal situations.

When comparing measurements of cirrus properties with simulations within the context of interpreting in-situ measurements or within a data assimilation setting it would be beneficial to capture contrail induced cirrus perturbations and the impact of pre-existing cirrus clouds on contrail formation. It can be expected that the large perturbations induced by contrail formation within natural cirrus lead to large modifications of cirrus microphysical and optical properties that need to be included in estimates of the aviation climate impact. Whether the impact of the pre-existing cirrus ice crystals on contrail formation would lead to a large change in the climate impact of contrail induced cirrus modifications is more difficult to answer.

We know that a very low percentage of contrails that form in cloud-free air explain a large part of the climate impact due to contrail cirrus (Burkhardt et al., 2018). We also know that whether contrails will have a large impact or not depends crucially on the synoptic situation (Bier et al., 2017) with large scale ice supersaturated areas, such as those connected with fronts, leading to large scale contrail cirrus outbreaks. Our study shows that in those large-scale ice supersaturated areas, e.g. connected with frontal systems, cirrus clouds may be significantly modified by contrail formation within pre-existing cirrus and the pre-existing cirrus can have a relatively large impact on the contrail ice nucleation and survival. Furthermore, the steady supply of moisture in the lifting zones is likely to lead to long life times of the contrail induced cirrus perturbations. Even though the impact of pre-existing cirrus on contrail formation is only infrequently large, long life times and large IWC of the cirrus modifications may make them radiatively important.



The pre-existing cirrus can lead to changes in the contrail formation criterion and, therefore, can lead to contrail formation when otherwise (in the absence of cirrus ice crystals) none would have formed. In those situations, only few ice crystals may form, i.e. few when compared to other contrails but possibly many when compared to natural cirrus clouds. That means that the pre-existing cirrus ice crystals can lead to contrail formation in cases when otherwise the passage of an airplane would have dissolved the cirrus. The contrail formation may then lead either to cirrus cloud properties not dissimilar to the properties of the natural cirrus or to significantly larger ice crystal numbers. What kind of impact the dissolution or the change in cirrus properties has on climate cannot be estimated merely from the statistics of contrail formation such as described in our study. Instead the processes described here need to be integrated in a climate model and the life cycle in contrail induced cirrus modifications need to be simulated and the associated change in radiative transfer estimated.

710

715 Building on the presented results regarding contrail formation within cirrus and the impact of pre-existing cirrus on the contrail formation, processes controlling the life cycle of the contrail induced cirrus perturbations and their impact on cirrus properties needs to be studied. Estimates of the climate impact of contrail formation within cirrus are required in order to complete current estimates of the climate impact of air traffic (Lee et al., 2021). A complete picture of the climate impact of air traffic including all the climate forcing components together with their uncertainties is crucially necessary for the evaluation of mitigation options that require calculating the tradeoffs between different climate forcing components. Finally, our work allows to improve the interpretation of cirrus observational data from flight campaigns and remote sensing and adds complexity to discussions about the importance of different ice nucleation pathways for cirrus properties.

720

### Code Availability

The ICON model is distributed to institutions under an institutional license issued by the DWD. Two copies of the institutional license need to be signed and returned to the DWD. ICON can be then downloaded at <https://data.dwd.de>. To individuals, the ICON model is distributed under a personal non-commercial research license distributed by the MPI-M (Max Planck Institute for Meteorology). Every person receiving a copy of the ICON framework code accepts the ICON personal non-commercial research license by doing so. Or, as the license states, any use of the ICON software is conditional upon and therefore leads to an implied acceptance of the terms of the Software License Agreement. To receive an individually licensed copy, please follow the instructions provided at [https://code.mpimet.mpg.de/projects/iconpublic/wiki/Instructions\\_to\\_obtain\\_the\\_ICON\\_model\\_code\\_with\\_a\\_personal\\_non-commercial\\_research\\_license](https://code.mpimet.mpg.de/projects/iconpublic/wiki/Instructions_to_obtain_the_ICON_model_code_with_a_personal_non-commercial_research_license).

725

730

### Data Availability

Data is used in the figures can be access from the given DOI: (Verma, 2021, <https://doi.org/10.5281/zenodo.4946601>)

735



### Author contributions

PV and UB jointly designed the study. PV have performed simulations and analyzed the results. PV and UB jointly discussed  
740 scientific results and wrote the manuscript.

### Competing interests

The authors declare that they have no conflict of interest.

### Acknowledgements

We gratefully acknowledge the HD(CP)2 project that performed the ICON-LEM simulations on which our study is based. We  
745 thank Jan Frederik Engels from DKRZ for technical help implementing the contrail scheme and the air traffic inventory in  
ICON-LEM. We thank Klaus Gierens, Andreas Schäffler and Simon Unterstrasser from DLR and Axel Seifert and Daniel  
Reinert from DWD and the whole HD(CP)2 community for valuable discussions. We thank Winfried Beer and Bastian Kern  
for their technical support at DLR.

### Financial support

750 This work is funded by the research program “High Definition of Clouds and Precipitation for Advancing Climate Prediction”  
(HD(CP)2) of the BMBF (German Federal Ministry of Education and Research) under grant 01LK1503C. The authors  
gratefully acknowledge the computing time granted by the German Climate Computing Centre (Deutsches  
Klimarechenzentrum, DKRZ, Hamburg, Germany).

### References

- 755 Baldauf, M. and Brdar, S.: 3D diffusion in terrain-following coordinates: testing and stability of horizontally explicit, vertically  
implicit discretizations, *Quarterly Journal of the Royal Meteorological Society*, 142(698), 2087–2101,  
<https://doi.org/10.1002/qj.2805>, 2016.
- 760 Bickel, M., Ponater, M., Bock, L., Burkhardt, U., and Reineke, S.: Estimating the Effective Radiative Forcing of Contrail  
Cirrus, *Journal of Climate*, 33(5), 1991–2005, <https://doi.org/10.1175/jcli-d-19-0467.1>, 2020.



- Bier, A. and Burkhardt, U.: Variability in Contrail Ice Nucleation and Its Dependence on Soot Number Emissions, *Journal of Geophysical Research: Atmospheres*, 124(6), 3384–3400, <https://doi.org/10.1029/2018jd029155>, 2019.
- 765 Bier, A., Burkhardt, U., and Bock, L.: Synoptic Control of Contrail Cirrus Life Cycles and Their Modification Due to Reduced Soot Number Emissions, *Journal of Geophysical Research: Atmospheres*, 122(21), 11,584–11,603, <https://doi.org/10.1002/2017jd027011>, 2017.
- Bock, L. and Burkhardt, U.: Reassessing properties and radiative forcing of contrail cirrus using a climate model, *Journal of Geophysical Research: Atmospheres*, 121(16), 9717–9736, <https://doi.org/10.1002/2016jd025112>, 2016. a
- 770
- Bock, L. and Burkhardt, U.: The temporal evolution of a long-lived contrail cirrus cluster: Simulations with a global climate model, *Journal of Geophysical Research: Atmospheres*, 121(7), 3548–3565, <https://doi.org/10.1002/2015jd024475>, 2016. b
- 775 Bock, L. and Burkhardt, U.: Contrail cirrus radiative forcing for future air traffic, *Atmospheric Chemistry and Physics*, 19(12), 8163–8174, <https://doi.org/10.5194/acp-19-8163-2019>, 2019.
- Boucher, O., D. Randall, P. Artaxo, C. Bretherton, G. Feingold, P. Forster, V.-M. Kerminen, Y. Kondo, H. Liao, U. Lohmann, P. Rasch, S.K. Satheesh, S. Sherwood, B. Stevens, and X.Y. Zhang, T.F. Stocker, D. Qin, G.-K. Plattner, M. Tignor, S.K. Allen, J. Doschung, A. Nauels, Y. Xia, V. Bex, and P.M. Midgley: Clouds and aerosols. In *Climate Change 2013: The Physical Science Basis, Contribution of Working Group I to the Fifth Assessment Report of the Intergovernmental Panel on Climate Change*, Eds. Cambridge University Press, pp. 571–657, <https://doi:10.1017/CBO9781107415324.016>, 2013.
- 780
- Bräuer, T., Voigt, C., Sauer, D., Kaufmann, S., Hahn, V., Scheibe, M., Schlager, H., Diskin, G. S., Nowak, J. B., DiGangi, J. P., Huber, F., Moore, R. H., and Anderson, B. E.: Airborne Measurements of Contrail Ice Properties - Dependence on Temperature and Humidity, *Geophysical Research Letters*, 1, <https://doi.org/10.1029/2020gl092166>, 2021.
- 785
- Burkhardt, U., Bock, L., and Bier, A.: Mitigating the contrail cirrus climate impact by reducing aircraft soot number emissions, *Npj Climate and Atmospheric Science*, 1(1), 37, <https://doi.org/10.1038/s41612-018-0046-4>, 2018.
- 790
- Burkhardt, U. and Kärcher, B.: Global radiative forcing from contrail cirrus, *Nature Climate Change*, 1(1), 54–58, <https://doi.org/10.1038/nclimate1068>, 2011.



795 Chen, C.-C. and Gettelman, A.: Simulated radiative forcing from contrails and contrail cirrus, *Atmospheric Chemistry and Physics*, 13(24), 12525–12536, <https://doi.org/10.5194/acp-13-12525-2013>, 2013.

800 Dipankar, A., Stevens, B., Heinze, R., Moseley, C., Zängl, G., Giorgetta, M., and Brdar, S.: Large eddy simulation using the general circulation model ICON, *Journal of Advances in Modeling Earth Systems*, 7(3), 963–986, <https://doi.org/10.1002/2015ms000431>, 2015.

Fichter, C., Marquart, S., Sausen, R., and Lee, D. S.: The impact of cruise altitude on contrails and related radiative forcing, *Meteorologische Zeitschrift*, 14(4), 563–572, <https://doi.org/10.1127/0941-2948/2005/0048>, 2005.

805 Gayet, J.-F., Febvre, G., Brogniez, G., Chepfer, H., Renger, W., and Wendling, P.: Microphysical and Optical Properties of Cirrus and Contrails: Cloud Field Study on 13 October 1989, *Journal of the Atmospheric Sciences*, 53(1), 126–138, [https://journals.ametsoc.org/view/journals/atsc/53/1/1520-0469\\_1996\\_053\\_0126\\_maopoc\\_2\\_0\\_co\\_2.xml](https://journals.ametsoc.org/view/journals/atsc/53/1/1520-0469_1996_053_0126_maopoc_2_0_co_2.xml), 1996.

Gerz, T., Dürbeck, T., and Konopka, P.: Transport and effective diffusion of aircraft emissions, *Journal of Geophysical Research: Atmospheres*, 103(D20), 25905–25913, <https://doi.org/10.1029/98jd02282>, 1998.

810 Gierens, K.: Selected topics on the interaction between cirrus clouds and embedded contrails, *Atmospheric Chemistry and Physics*, 12(24), 11943–11949, <https://doi.org/10.5194/acp-12-11943-2012>, 2012.

815 Gruber, S., Unterstrasser, S., Bechtold, J., Vogel, H., Jung, M., Pak, H., & Vogel, B.: Contrails and their impact on shortwave radiation and photovoltaic power production – a regional model study, *Atmospheric Chemistry and Physics*, 18(9), 6393–6411, <https://doi.org/10.5194/acp-18-6393-2018>, 2018.

820 Hande, L. B., Engler, C., Hoose, C., and Tegen, I.: Parameterizing cloud condensation nuclei concentrations during HOPE, *Atmospheric Chemistry and Physics*, 16(18), 12059–12079, <https://doi.org/10.5194/acp-16-12059-2016>, 2016.

825 Heinze, R., Dipankar, A., Henken, C. C., Moseley, C., Sourdeval, O., Trömel, S., Xie, X., Adamidis, P., Ament, F., Baars, H., Barthlott, C., Behrendt, A., Blahak, U., Bley, S., Brdar, S., Brueck, M., Crewell, S., Deneke, H., Di Girolamo, P., Evaristo, R., Fischer, J., Frank, C., Friederichs, P., Göcke, T., Gorges, K., Hande, L., Hanke, M., Hansen, A., Hege, H.-C., Hoose, C., Jahns, T., Kalthoff, N., Klocke, D., Kneifel, S., Knippertz, P., Kuhn, A., van Laar, T., Macke, A., Maurer, V., Mayer, B., Meyer, C. I., Muppa, S. K., Neggers, R. A. J., Orlandi, E., Pantillon, F., Pospichal, B., Röber, N., Scheck, L., Seifert, A., Seifert, P., Senf, F., Siligam, P., Simmer, C., Steinke, S., Stevens, B., Wapler, K., Weniger, M., Wulfmeyer, V., Zängl, G., Zhang, D., and



- Quaas, J.: Large-eddy simulations over Germany using ICON: a comprehensive evaluation, *Q. J. Roy. Meteor. Soc.*, 143, 69–100, <https://doi.org/10.1002/qj.2947>, 2017.
- 830 Kapadia, Z. Z., Spracklen, D. V., Arnold, S. R., Borman, D. J., Mann, G. W., Pringle, K. J., Monks, S. A., Reddington, C. L., Benduhn, F., Rap, A., Scott, C. E., Butt, E. W., and Yoshioka, M.: Impacts of aviation fuel sulfur content on climate and human health, *Atmospheric Chemistry and Physics*, 16(16), 10521–10541, <https://doi.org/10.5194/acp-16-10521-2016>, 2016.
- Kärcher, B., Burkhardt, U., Bier, A., Bock, L., and Ford, I. J.: The microphysical pathway to contrail formation, *Journal of Geophysical Research: Atmospheres*, 120(15), 7893–7927, <https://doi.org/10.1002/2015jd023491>, 2015.
- 835 Kärcher, B., Hendricks, J., and Lohmann, U.: Physically based parameterization of cirrus cloud formation for use in global atmospheric models, *Journal of Geophysical Research*, 111(D1), 1, <https://doi.org/10.1029/2005jd006219>, 2006.
- 840 Kärcher, B. and Yu, F.: Role of aircraft soot emissions in contrail formation. *Geophysical Research Letters*, 36(1), 1, <https://doi.org/10.1029/2008gl036649>, 2009.
- Köhler, C. G. and Seifert, A.: Identifying sensitivities for cirrus modelling using a two-moment two-mode bulk microphysics scheme, *Tellus B: Chemical and Physical Meteorology*, 67(1), 24494, <https://doi.org/10.3402/tellusb.v67.24494>, 2015.
- 845 Lee, D. S., Fahey, D. W., Skowron, A., Allen, M. R., Burkhardt, U., Chen, Q., Doherty, S. J., Freeman, S., Forster, P. M., Fuglestvedt, J., Gettelman, A., De León, R. R., Lim, L. L., Lund, M. T., Millar, R. J., Owen, B., Penner, J. E., Pitari, G., Prather, M. J., Sausen, R., Wilcox, L. J.: The contribution of global aviation to anthropogenic climate forcing for 2000 to 2018, *Atmospheric Environment*, 244, 117834, <https://doi.org/10.1016/j.atmosenv.2020.117834>, 2021.
- 850 Lewellen, D. C., Meza, O., and Huebsch, W. W.: Persistent Contrails and Contrail Cirrus. Part I: Large-Eddy Simulations from Inception to Demise, *Journal of the Atmospheric Sciences*, 71(12), 4399–4419, <https://doi.org/10.1175/jas-d-13-0316.1>, 2014.
- Liou, K. N.: Influence of Cirrus Clouds on Weather and Climate Processes: A Global Perspective, *Monthly Weather Review*, 114(6), 1167–1199, [https://doi.org/10.1175/1520-0493\(1986\)114<1167:IOCCOW>2.0.CO;2](https://doi.org/10.1175/1520-0493(1986)114<1167:IOCCOW>2.0.CO;2), 1986.
- 855 Macke, A., Seifert, P., Baars, H., Barthlott, C., Beekmans, C., Behrendt, A., Bohn, B., Brueck, M., Bühl, J., Crewell, S., Damian, T., Deneke, H., Düsing, S., Foth, A., Di Girolamo, P., Hammann, E., Heinze, R., Hirsikko, A., Kalisch, J., Kalthoff, N., Kinne, S., Kohler, M., Löhnert, U., Madhavan, B. L., Maurer, V., Muppa, S. K., Schween, J., Serikov, I., Siebert, H., 860 Simmer, C., Späth, F., Steinke, S., Träumner, K., Trömel, S., Wehner, B., Wieser, A., Wulfmeyer, V., and Xie, X.: The





- HD(CP)<sup>2</sup> Observational Prototype Experiment (HOPE) – an overview, *Atmos. Chem. Phys.*, 17, 4887–4914, <https://doi.org/10.5194/acp-17-4887-2017>, 2017.
- Matthes, S., Lim, L., Burkhardt, U., Dahlmann, K., Dietmüller, S., Grewe, V., Haslerud, A. S., Hendricks, J., Owen, B., Pitari, G., Righi, M., and Skowron, A.: Mitigation of Non-CO<sub>2</sub> Aviation's Climate Impact by Changing Cruise Altitudes, *Aerospace*, 8(2), 36, <https://doi.org/10.3390/aerospace8020036>, 2021.
- Paoli, R. and Shariff, K.: Contrail Modeling and Simulation, *Annual Review of Fluid Mechanics*, 48(1), 393–427, <https://doi.org/10.1146/annurev-fluid-010814-013619>, 2016.
- Pruppacher, H. R. and Klett, J. D. (1996). *Microphysics of Clouds and Precipitation* (Atmospheric and Oceanographic Sciences Library (18)) (2nd ed. 2010 ed.), Kluwer Academic Publishers, Dordrecht, the Netherlands, 1997.
- Ramanathan, V., Cess, R. D., Harrison, E. F., Minnis, P., Barkstrom, B. R., Ahmad, E., & Hartmann, D.: Cloud-Radiative Forcing and Climate: Results from the Earth Radiation Budget Experiment, *Science*, 243(4887), 57–63, <https://doi.org/10.1126/science.243.4887.57>, 1989.
- Righi, M., Hendricks, J., and Sausen, R.: The global impact of the transport sectors on atmospheric aerosol: simulations for year 2000 emissions, *Atmospheric Chemistry and Physics*, 13(19), 9939–9970, <https://doi.org/10.5194/acp-13-9939-2013>, 2013.
- Ruppert T.: Vector field reconstruction by radial basis functions, Master's thesis. Department of Mathematics, Technical University Darmstadt: Darmstadt., 2007.
- Schröder, F., Kärcher, B., Duroure, C., Ström, J., Petzold, A., Gayet, J.-F., Strauss, B., Wendling, P., and Borrmann, S.: On the Transition of Contrails into Cirrus Clouds, *Journal of the Atmospheric Sciences*, 57(4), 464–480, [http://www.pa.op.dlr.de/~BerndKaercher/JAS57\\_464-480\\_2000.pdf](http://www.pa.op.dlr.de/~BerndKaercher/JAS57_464-480_2000.pdf)., 2000.
- Schumann, U.: On conditions for contrail formation from aircraft exhausts, *Meteorologische Zeitschrift*, 5(1), 4–23. <https://doi.org/10.1127/metz/5/1996/4>, 1996.
- Schumann, U. and Heymsfield, A. J.: On the Life Cycle of Individual Contrails and Contrail Cirrus, *Meteorological Monographs*, 58, 3.1–3.24, <https://doi.org/10.1175/amsmonographs-d-16-0005.1>, 2017.



895 Schumann, U., Penner, J. E., Chen, Y., Zhou, C., and Graf, K.: Dehydration effects from contrails in a coupled contrail–climate model, *Atmospheric Chemistry and Physics*, 15(19), 11179–11199, <https://doi.org/10.5194/acp-15-11179-2015>, 2015.

Seifert, A. and Beheng, K. D.: A two-moment cloud microphysics parameterization for mixed-phase clouds. Part 1: Model description, *Meteorology and Atmospheric Physics*, 92(1–2), 45–66, <https://doi.org/10.1007/s00703-005-0112-4>, 2006.

900

Stevens, B., and Bony, S.: What Are Climate Models Missing? *Science*, 340(6136), 1053–1054, <https://doi.org/10.1126/science.1237554>, 2013.

Stevens, B., Acquistapace, C., Hansen, A., Heinze, R., Klinger, C., Klocke, D., Rybka, H., Schubotz, W., Windmiller, J.,  
905 Adamidis, P., Arka, I., Barlakas, V., Biercamp, J., Brueck, M., Brune, S., Buehler, S. A., Burkhardt, U., Cioni, G., Costa-  
Surós, M., Crewell, S., Crüger, T., Deneke, H., Friederichs, P., Henken, C. C., Hohenegger, C., Jacob, M., Jakub, F., Kalthoff,  
N., Köhler, M., van Laar, T. W., Li, P., Löhnert, U., Macke, A., Madenach, N., Mayer, B., Nam, C., Naumann, A. K., Peters,  
K., Poll, S., Quaas, J., Röber, N., Rochetin, N., Scheck, L., Schemann, V., Schnitt, S., Seifert, A., Senf, F., Shapkalijevski, M.,  
Simmer, C., Singh, S., Sourdeval, O., Spickermann, D., Strandgren, J., Tessiot, O., Vercauteren, N., Vial, J., Voigt, A., and  
910 Zängl, G.: The Added Value of Large-Eddy and Storm-Resolving Models for Simulating Clouds and Precipitation, *J. Meteorol.*  
*Soc. Jpn.*, 98, 395–435, <https://doi.org/10.2151/jmsj.2020-021>, 2020.

Tesche, M., Aichtert, P., Glantz, P., and Noone, K. J.: Aviation effects on already-existing cirrus clouds, *Nature Communications*, 7(1), 1, <https://doi.org/10.1038/ncomms12016>, 2016.

915

Unterstrasser, S.: Large-eddy simulation study of contrail microphysics and geometry during the vortex phase and consequences on contrail-to-cirrus transition, *Journal of Geophysical Research: Atmospheres*, 119(12), 7537–7555, <https://doi.org/10.1002/2013jd021418>, 2014.

920 Unterstrasser, S.: Properties of young contrails – a parametrisation based on large-eddy simulations, *Atmospheric Chemistry and Physics*, 16(4), 2059–2082, <https://doi.org/10.5194/acp-16-2059-2016>, 2016.

Voigt, C., Schumann, U., Minikin, A., Abdelmonem, A., Afchine, A., Borrmann, S., Boettcher, M., Buchholz, B., Bugliaro, L., Costa, A., Curtius, J., Dollner, M., Dörnbrack, A., Dreiling, V., Ebert, V., Ehrlich, A., Fix, A., Forster, L., Frank, F.,  
925 Fütterer, D., Giez, A., Graf, K., Groß, J.-U., Groß, S., Heimerl, K., Heinold, B., Hüneke, T., Järvinen, E., Jurkat, T., Kaufmann, S., Kenntner, M., Klingebiel, M., Klimach, T., Kohl, R., Krämer, M., Krisna, T. C., Luebke, A., Mayer, B., Mertes, S., Molléker, S., Petzold, A., Pfeilsticker, K., Port, M., Rapp, M., Reutter, P., Rolf, C., Rose, D., Sauer, D., Schäfler, A., Schlage, R., Schnaiter, M., Schneider, J., Spelten, N., Spichtinger, P., Stock, P., Walser, A., Weigel, R., Weinzierl, B.,



- 930 Wendisch, M., Werner, F., Wernli, H., Wirth, M., Zahn, A., Ziereis, H., and Zöger, M.: ML-CIRRUS – The airborne  
experiment on natural cirrus and contrail cirrus with the high-altitude long-range research aircraft HALO, *B. Am. Meteorol.  
Soc.*, 98, 271–288, <https://doi.org/10.1175/BAMS-D-15-00213.1>, 2017.
- 935 Wan, H., Giorgetta, M. A., Zängl, G., Restelli, M., Majewski, D., Bonaventura, L., Fröhlich, K., Reinert, D., Rípodas, P.,  
Kornbluh, L., and Förstner, J.: The ICON-1.2 hydrostatic atmospheric dynamical core on triangular grids – Part 1:  
Formulation and performance of the baseline version, *Geoscientific Model Development*, 6(3), 735–763,  
<https://doi.org/10.5194/gmd-6-735-2013>, 2013.
- 940 Wilkerson, J. T., Jacobson, M. Z., Malwitz, A., Balasubramanian, S., Wayson, R., Fleming, G., Naiman, A. D., and Lele, S.  
K.: Analysis of emission data from global commercial aviation: 2004 and 2006, *Atmospheric Chemistry and Physics*, 10(13),  
6391–6408, <https://doi.org/10.5194/acp-10-6391-2010>, 2010.
- 945 Wolke, R., Knoth, O., Hellmuth, O., Schröder, W., and Renner, E.: The parallel model system LM-MUSCAT for chemistry-  
transport simulations: Coupling scheme, parallelization and applications, *Advances in Parallel Computing*, 363–369,  
[https://doi.org/10.1016/s0927-5452\(04\)80048-0](https://doi.org/10.1016/s0927-5452(04)80048-0), 2004.
- 950 Wolke, R., Schröder, W., Schrödner, R., and Renner, E.: Influence of grid resolution and meteorological forcing on simulated  
European air quality: A sensitivity study with the modeling system COSMO–MUSCAT, *Atmospheric Environment*, 53, 110–  
130, <https://doi.org/10.1016/j.atmosenv.2012.02.085>, 2012.
- 955 Zängl, G., Reinert, D., Rípodas, P., & Baldauf, M.: The ICON (ICOsahedral Non-hydrostatic) modelling framework of DWD  
and MPI-M: Description of the non-hydrostatic dynamical core, *Quarterly Journal of the Royal Meteorological Society*,  
141(687), 563–579, <https://doi.org/10.1002/qj.2378>, 2014.
- Zhang, Y., Macke, A., & Albers, F.: Effect of crystal size spectrum and crystal shape on stratiform cirrus radiative forcing,  
*Atmospheric Research*, 52(1–2), 59–75, [https://doi.org/10.1016/s0169-8095\(99\)00026-5](https://doi.org/10.1016/s0169-8095(99)00026-5), 1999.